6-28-2018

An Evaluation of the Utility of a Mass-Weighted Frequency Distribution of Sediment for Modeling Aeolian Transport Rates

Raihan Jamil
Louisiana State University and Agricultural and Mechanical College, rjamil.kuet@gmail.com

AN EVALUATION OF THE UTILITY OF A MASS-WEIGHTED FREQUENCY DISTRIBUTION OF SEDIMENT FOR MODELING AEOLIAN TRANSPORT RATES

A Thesis

Submitted to the Graduate Faculty of the
Louisiana State University and
Agricultural and Mechanical College
in partial fulfillment of the
requirements for the degree of
Master of Science

in

The Department of Geography and Anthropology

by
Raihan Jamil
Bachelor, Khulna University of Engineering and Technology, Bangladesh, 2015
August 2018

ACKNOWLEDGEMENTS

It is a great privilege to express my deepest and sincere appreciation to my advisor and mentor Dr. Steven L. Namikas. His kind, constant encouragement, direction, support, and advice provided me the inspiration and strength to accomplish this work.

I would like to thank my graduate committee member Dr. Barry D. Keim and Dr. Kory Konsoer for their support and guidance throughout my research and studies. I also would like to thank the LSU faculty, particularly Dr. Shelly Meng and Ms. Erika DeLeon, my colleagues, in addition to and classmates, especially Taylor Rowley for their information, encouragement, insightful reviews and feedback. I am thankful to everyone who has supported me in conducting this research directly and indirectly. I would like to give thanks to all the awesome members of the LSU Bangladeshi Students' Association for their wonderful, warm and cordial conducts.

I am grateful to my parents, sisters, teachers, friends, and relatives for their motivations, best wishes, and support. I always find them beside me in any of my crises and hardships and they provide me the strength to move on. Finally, all praise is due to the Almighty, who has blessed me with His mercy.

TABLE OF CONTENTS

LIST OF TABLES

LIST OF FIGURES

ABSTRACT

Predictions made by aeolian transport models often do not match well with measured data. The poor predictive capability of these models remains a fundamental problem in aeolian geomorphology. This study evaluates the effectiveness of the recently proposed mass-weighted frequency distribution (Edwards and Namikas 2015) and the apparent von Kármán parameter proposed by Li et al. (2010) to improve transport rate predictions. The evaluation consists of comparisons of predicted transport rates versus a large dataset of measured field and lab transport rates collected from the literature. The transport rate predictions are made both with and without recalibration of model empirical coefficients. The mass-weighted frequency distribution produces a small but statistically significant degree of improvement in agreement between observed and predicted transport rates. The greatest increase in R^2 value occurs with the Hsu (1971) model (from 0.485 to 0.564). The disparity in predictions between different models is also reduced significantly. Use of the apparent von Kármán parameter is found to be limited to a particular range of sediment transport rates ($Q < 0.028$ $kgm^{-1}s^{-1}$). The apparent von Kármán parameter provides the largest degree of predictive improvement with the Kadib (1965) model.

CHAPTER 1: INTRODUCTION

1.1. Problem Statement

In many field experiments it has been observed that predictions made by aeolian transport rate models do not agree well with measured data (Berg 1983, Horikawa et al. 1986, Sarre 1988, Chapman 1990, McEwan and Willetts 1994, Sherman et al. 1998, Dong et al. 2004, Liu et al. 2006, Bauer et al. 2009, Sherman and Li 2012). The poor predictive capabilities of these models remain a fundamental problem in aeolian geomorphology (Baas 2007, Bauer et al. 2009, Ellis et al. 2012, Kok et al. 2012, Kok et al. 2014)). As well, available models produce a wide range of predicted transport for a given set of conditions (Figure 1). This study seeks to address this problem by incorporating a more realistic approach to representing the local sediment size distribution, and by employing a new parameterization of the von Kármán constant, in commonly used models of the aeolian transport rate.

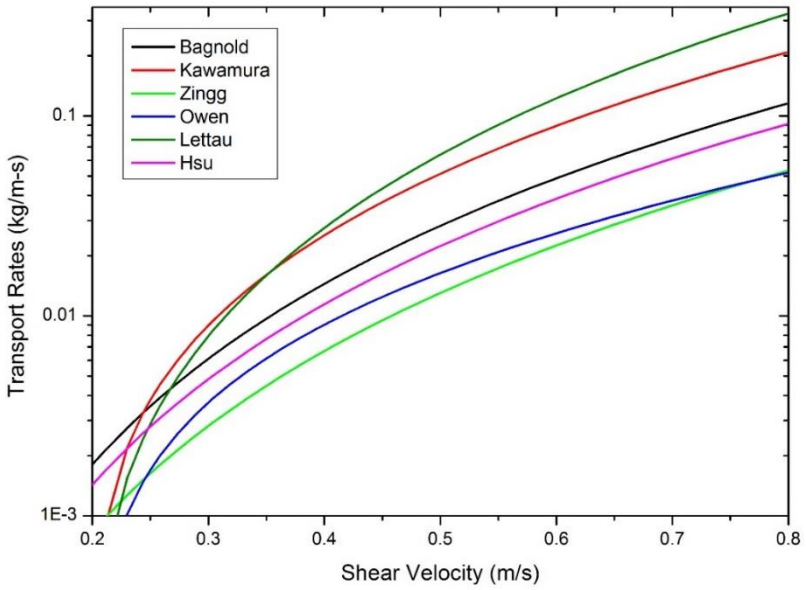

Figure 1: Range in predictions for commonly used models of aeolian transport. Calculations are based on a mean grain diameter of 0.25 mm.

As shown in Figure 2, predicted transport rates are typically larger than observed rates (Berg 1983, Horikawa et al. 1986, Sarre 1988, Chapman 1990, McEwan and Willetts 1994, Sherman et al. 1998, Dong et al. 2004, Liu et al. 2006, Bauer et al. 2009, Sherman and Li 2012).

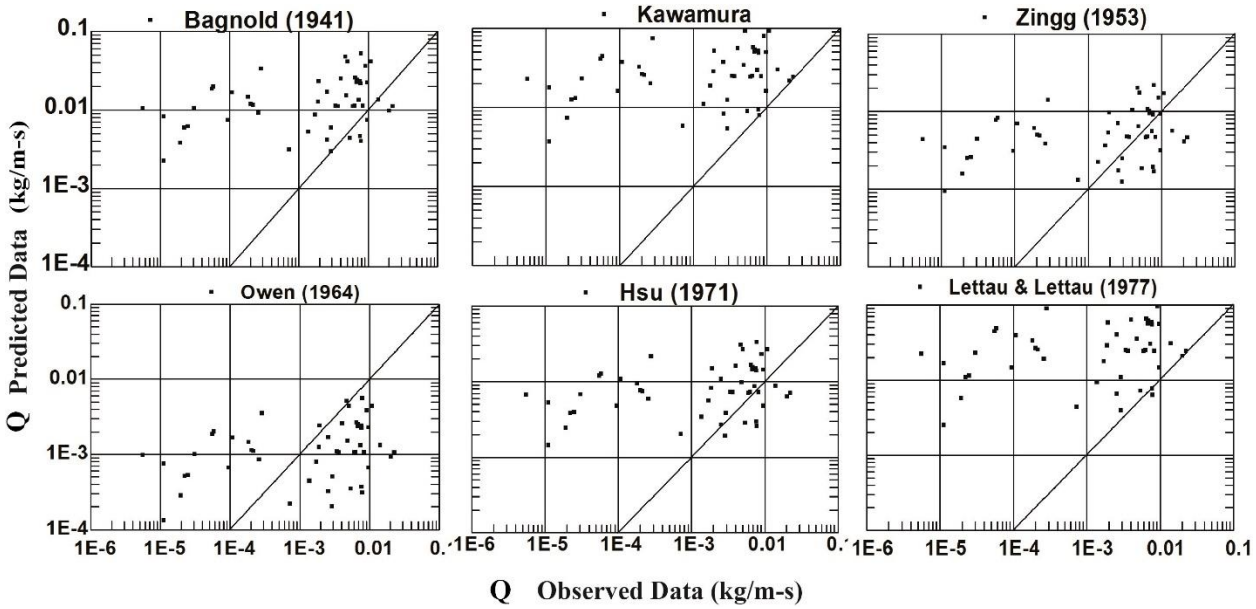

Figure 2: Example of over-prediction in comparison of predicted and measured transport rates. Data from Sherman et al. (1998).

This problem is generally attributed in part to site-specific environmental characteristics that are not included in the models. For example, although natural beaches are composed of a range of grain sizes with varying degrees of sorting (Horikawa et al. 1986, Sherman et al. 1998, Dong et al. 2003, Neuman 2003, Liu et al. 2006, Sherman and Li 2012), all aeolian transport models employ a single average grain diameter to represent the sediment bed (Bagnold 1936, Kawamura 1951, Owen 1964, Kadib 1965, Leatherman 1978). The traditional modeling approach determines this representative grain size based on the distribution of grain diameters present. However, the distribution of inertial forces resisting motion is not linearly proportional to the distribution of grain diameters, so that a diameter based mean may not adequately represent the distribution of the resisting forces (Edwards and Namikas 2015).

To more closely approximate the actual resistance to motion of the particles that comprise the local bed, Edwards and Namikas (2015) developed a mass-weighted size distribution of the sediment population. In this approach, the standard diameter-weighted frequency distribution is transformed to a mass-weighted frequency distribution that provides an improved approximation of the resistance to motion present in the bed. This approach was found to substantively enhance the agreement of threshold shear velocity predictions with a dataset of measurements derived from the literature (Edwards and Namikas, 2015). The present study extends this work by incorporating the new sediment size representation into models of the aeolian transport rate.

A second component that is common to virtually all attempts to model aeolian transport is use of a constant value for the von Kármán parameter in shear velocity calculations. However, in field experiments, Li et al. (2010) found that as the transport rate increases, the value of the von Kármán parameter appears to decrease. Based on this finding Li et al. (2010) proposed an 'apparent' von Kármán parameter that varies as a function of the transport rate. This project also investigates the utility of the apparent von Kármán constant in improving the fit between observed and predicted sediment transport rates.

1.2. Research Objectives

This study seeks to accomplish the following specific objectives:

A. Assess the ability of a mass-weighted frequency distribution of sediment to improve aeolian sediment transport predictions.

B. Evaluate use of the apparent von Kármán constant in improving the fit between observed and predicted aeolian transport rates.

1.3 Broader Significance of the Reseach

Aeolian sediment transport contributes to a wide range of socially relevant problems. These problems include crop damage resulting from abrasion and burial in the sand (Armbrust and Retta 2000, Skidmore 1966), loss of water storage capacity for plants (Field et al. 2010), and degradation of soil structure in agricultural fields (Fryrear and Downes 1975, Sterk 2003). Crop damage ranges from reduced growth and development to a total destruction of crops (Michels et al. 1995, Rinaudo 1996). A second problem is soil degradation caused by the loss of topsoil, which has an impact on the physical and chemical properties of the soil. The removal of fine particles results in a deterioration of soil structure. The texture of an actively eroding soil becomes progressively coarser, which negatively affects structure stability and water-holding capacity (Lal 1988, Sterk 2000). Aeolian processes affect roughly 430 million hectares of agricultural land worldwide (UNEP 1999). Further, an average of 1.7 million hectares of lands are damaged annually in the U.S. great plains region by wind erosion (Fryrear, 1981). Aeolian processes are considered to have contributed to more than 40% of degraded agricultural land (Middleton and Thomas 1997).

Aeolian sediment transport and the resulting formation and migration of sand dunes also pose varying degrees of risk to human infrastructure, ranging from the inconvenience and costs of sand blown into buildings or machinery to large-scale inundation of villages by migrating dunes (Sherman and Nordstrom 1994). Wind-blown sand and migrating dunes are capable of invading forests (Madore and Leatherman 1981, Barrere 1992); burying roads and railways (Kellogg 1915), inundating cemeteries and recreational areas (Draga 1983, Granja and Carvalho 1992), and reducing visibility and causing physical discomfort.As a natural disaster, wind-blown sand is certainly less dramatic than tsunami, earthquakes, hurricanes and floods. However, the cost of

remediation is high and the resulting societal implications are great (Sherman and Nordstrom 1994).

In summary, a potential for harmful impacts from blowing sand exists at virtually every sandy coastline, arid and semi-arid region. A better understanding of the basic physical process of wind-blown sand is a prerequisite for the development of more accurate predictive model of sand transport, and for comprehensive environmental management approaches aimed at mitigating aeolian hazards. This study will contribute to improving our understanding of the basic physics of aeolian sediment transport, which will in turn allow for improvements in modeling and managing the impacts of aeolian processes.

CHAPTER 2: LITERATURE REVIEW

In this chapter, the following topics are addressed. First, the aeolian transport models employed in the study are outlined. This section is continued by comparing the performance of these models outlined in previous field and wind tunnel experiments. Second, the mass-weighted frequency distribution developed by Edwards and Namikas (2015), and the apparent von Kármán approach proposed by Li et al. (2010) are outlined. Finally, site specific complications of aeolian transport models are discussed briefly.

2. 1 Aeolian Transport Models

The most widely used aeolian transport models have typically been generated from a physical/mechanical perspective, balancing the energy required to move a given amount of sand with the energy available from the wind field. Most relate the transport rate (Q) to the third power of shear velocity (u_*). To improve compatibility between measured and observed transport rates, and account for unknowns and errors associated with simplifications, all aeolian transport models include one or more empirical coefficients. These are typically derived from best-fits of a model to wind tunnel or field measurements (Gerety 1985, McEwan and Willetts 1994, Arnold 2002, Bauer et al. 2004, Farrell and Sherman 2006, Sherman and Farrell 2008, Sherman and Li 2012).

The following aeolian transport models represent the approaches most commonly employed in the literature, and are those which have been selected for use in this study.

2.1.1 Bagnold (1937) proposed the first physically based relation:

$$Q = C_B \sqrt{\frac{d}{D}} \frac{\rho}{g} u_*^3 \quad \text{..... (1)}$$

where d is the mean grain diameter, D is a reference grain diameter with a value of 0.25 mm (Bagnold 1937), ρ is air density, g is gravitational acceleration, and C_B is an empirical coefficient (which Bagnold suggested ranges in value from 1.5 to 2.8 with a value of 1.8 for naturally graded sand).

This was the first physically based aeolian transport model. In contrast, O'Brien and Rindlaub (1936) represented the state of the art at that time - an empirical fit of several field-measured transport rates to co-located wind velocity measurements. The Bagnold model represents the first attempt at a generally applicable model. It also remains the most widely used approach. This relation is technically only suitable for wind speeds above the threshold of motion, as the predicted transport rates do not go to zero at lower speeds (Svasek and Terwindt 1974, Herrmann 2000, Li et al. 2009). This model predicts lower transport rates than those of the Kawamura (1951) equation at high wind shear and generally provides an intermediate estimate of transport rates (Fig. 1). Sherman et al. (1998) found this model to be moderately effective, while Sherman and Li (2012) found it to be the most effective in predicting aeolian sediment transport rates (with the use of the apparent von Kármán parameter modification).

Bagnold (1936) conducted his experiments in a wind tunnel that had the ability to receive sand during operation. Wind velocities were measured using a small pitot tube with an internal diameter of 0.8 mm. Sand transport was measured using balances to determine accumulation or loss of sand from the working sections. The study included six runs with shear velocities ranging from 0.19 to 0.88 ms^{-1}. The sand used was pre-sieved and included a narrow grain size range of 0.18 to 0.30 mm. The measured transport rates ranged from 0.0029 to 0.122 $kgm^{-1}s^{-1}$.

2.1.2 Kawamura (1951) proposed the relation:

$$Q=C_K \frac{\rho}{g} (u_* - u_{*t}) (u_* + u_{*t})^2 \quad \ldots\ldots (2)$$

where C_k is an empirical coefficient and u_{*t} is the threshold shear velocity. Kawamura obtained a value of C_k =2.78 based on wind tunnel experiments, but subsequent research has suggested that C_k is closer to 2.3 in some environments (Horikawa et al. 1984, Sarre 1988).

This model is less directly dependent on grain size than most other models, although grain size is indirectly incorporated it in the threshold shear velocity term. Kawamura (1951) represented a significant theoretical advance as it was the first model to include an explicit threshold shear velocity term. One advantage of this approach is that it prevents spurious predictions of sand transport when shear velocity is less than the threshold velocity. Kawamura (1951) conducted both field and laboratory experiments. However, he used only the laboratory data to define the value of C_k. He used natural beach sand with a 0.25 mm mean grain size for the experiments.

The Kawamura (1951) model typically produces the upper range of predicted transport rates, particularly at higher shear velocities (Figure 1). Sarre (1988) found this model to provide the best fit to measurements collected in the intertidal zone. Svasek and Terwindt (1974) also found that the model of Kawamura provided the best representation of their field data.

Threshold shear velocity is commonly modeled following Bagnold (1936) as:

$$u_{*t}=A \sqrt{\frac{\rho_s - \rho}{\rho_a} g d_{50}} \quad \ldots\ldots (3)$$

where ρ_S is the density of sediment and A is a dimensionless coefficient usually taken as 0.085. This equation is based on consideration of the balance of forces acting on the particle that will be just sufficient to set it in motion. This approach will be employed for threshold calculations here.

2.1.3 Zingg (1953) proposed the relation:

$$Q=C_Z \left(\frac{d}{D}\right)^{\frac{3}{4}} \frac{\rho}{g} u_*^{\,3} \quad \text{.....(4)}$$

where C_Z is an empirical coefficient with a value of 0.83. This model is similar to Bagnold (1936) but introduced a 3/4 power function of the grain diameter instead of original 1/2 power, and a smaller value for the empirical coefficient.

Owen (1964) noted that the Zingg's calibration experiment covered a wider range of particle sizes than those of Bagnold, which justified the use of a 3/4 power function. This model predicts transport rates towards the smaller end over most of the shear velocity range (Figure 1). Sherman et al. (2013) found this model to produce the greatest correspondence with their observations of transport rates, when the regression line was forced through zero.

Zingg (1953) employed a portable wind tunnel to calibrate the model. Five sizes of quartz sand were used for the experiments: 0.20, 0.275, 0.36, 0.505, and 0.715 mm. The grains were well-rounded, smooth, and approximately spherical in shape. Wind velocities were measured above a point near the center of the shear tray by use of small pitot tube. Transport was measured using dust samplers which were designed from commercial vacuum cleaners. Zingg (1953) conducted a total of 43 experiments of two minutes in duration. The model was derived using multiple regression equations that had a correlation coefficient of 0.977.

2.1.4 Owen (1964) noted that Bagnold answered two questions imperfectly: 1) What is the effect of the saltation on the airflow at large distances from the surface? 2) What determines the concentration of particles engaging in the saltation? Owen tried to address the above two questions through the following model:

$$Q=(C_o+\frac{w_s}{3u_*})(1-\frac{u_{*t}^2}{u_*^2})(\frac{\rho u_*^3}{g}) \quad \text{..... (5)}$$

Where C_o is an empirical coefficient with a value of 0.25 and w_s is the terminal fall velocity of the mean grain size. Owen (1964) used data from Bagnold (1936) and Zingg (1953) to derive the value of empirical coefficient. The present study will follow Chen and Fryrear (2001) in calculating w_s as:

$$w_s=-0.775352+4.52645\sqrt{d} \quad \text{.....(6)}$$

The Owen (1964) model typically produces the lowest predicted transport rates (Figure 1).

2.1.5. Kadib (1965) proposed the model:

$$Q=\Phi\rho_s g\sqrt{\frac{(\rho_s-\rho)}{\rho u_*^2}gd^3} \quad \text{..... (7).}$$

where Φ is a transport intensity function, following Einstein (1950). This 'intensity of sediment transport' includes the flow intensity parameters ψ and ψ_*, as well as grain impact and grain screening factors, I and ε. Kadib (1965) provided graphical techniques to develop relationship of ε/I to ψ and ψ_* to Φ. The relationship has been developed using the following equation:

$$\frac{A_*\Phi}{1+A_*\Phi}=\frac{1}{\sqrt{2\pi}}\int_{B_*\psi_*-\frac{1}{\eta_0}}^{\infty}e^{-\frac{z^2}{2}}dz \quad \text{..... (8).}$$

where η_0 = 0.5 (Einstein and El-Samni 1949), A_*=43.5, B_*=0.143 (Einstein 1950), and z is the probability integral and can be selected from a table. The value of ψ_* is derived from the following expression:

$$\psi_*=\psi\frac{\varepsilon}{I} \quad \text{..... .....(9)}$$

and ψ can be obtained from:

$$\psi = \frac{(\rho_s - \rho)gD}{\rho u_*^2} \quad \text{.....(10)}$$

Kadib (1965) essentially expanded Bagnold's original model through inclusion of portions of Einstein (1950) fluvial transport equation**.** The value of Φ varies with shear velocity and this may help to eliminate the simplification of using a constant value for the empirical coefficient. The Kadib (1965) model provides the upper range of predictions when shear velocity is less than about 0.30 ms^{-1}, but it provides the lower range when shear velocity is greater than 0.50 ms^{-1}.

To verify this relationship, Kadib (1965) conducted a wind tunnel experiment using relatively coarse sand (0.88 to 1 mm). Wind velocities were measured using a standard Prandtl type Pitot tube. To feed sand into the wind tunnel automatically, a hopper was used near the entrance to the tunnel. The sand surface was well mixed after each run to remove any effect of sorting. The shear velocity was varied from 0.19 to 1.08 ms^{-1}. Berg (1983) found this model to provide the best fit to transport rates measured in a coastal dune complex.

2.1.6. Hsu (1971) proposed the relation:

$$Q = C_H \left(\frac{u_*}{\sqrt{gD}}\right)^3 \quad \text{..... (11)}$$

Hsu (1971) identified the value of the empirical coefficient C_H through a best-fit relation with grain size:

$$\ln (C_H .10^4) = -0.47+4.97\ d \quad \text{..... (12).}$$

Hsu (1971) developed this model synthesizing and reinterpreting the work of other investigators and scaling the transport rate with a 'special Froude' number. This Froude number is a function of shear velocity, gravitational acceleration, and mean grain size of the sand particles. Later, the relationship was verified utilizing data from various natural environments. Predictions from this

model are similar to Bagnold (1936) but provide slightly smaller transport rates at all shear velocities. Unlike all the other expressions that include the effect of grain size, this model predicts reduced sand transport rates with an increase in grain diameter up to a size of 0.30 mm (Sarre 1988). It then follows the usual expectation of an increase in rates with increasing grain size for grains of diameters larger than 0.3 mm.

2.1.7. Lettau and Lettau (1978) proposed the relation:

$$Q=C_L \sqrt{\frac{d}{D}} \frac{\rho}{g} (u_* - u_{*t})\, u_*{}^2 \quad \text{.....(13)}$$

where, C_L is an empirical coefficient, commonly set as 4.2 (Lettau and Lettau, 1977), although higher values have been reported in other studies ranging from 4.7 to 9.9 (Liu et al. 2012, Dong and Wang, 2006, Wippermann and Gross 1986, Sherman et al. 2013).

This model predicts slightly larger transport rates than the Bagnold equation at higher shear velocities, but intermediate rates over most of the range. The inclusion of a threshold term removes the apparent inaccuracy of predicting sand movement below the threshold velocity. Measured transport rates within the intertidal zone were found to be estimated well by this model (Berg 1983, Sarre 1988). After recalibration using the apparent von Kármán parameter and forcing the least-squares line through the origins of the axes, Sherman et al. (2013) found this model to be the best for replicating transport rates observed in their field experiment.

Lettau and Lettau (1977) wanted to develop a method to approximate historic wind velocities from the migration rates of barchan dunes. Consequently, they developed a transport model as a component of that study. They conducted a field experiment on the crest of a barchan dune installing one anemometer at 0.63 m above the bed. Lettau and Lettau (1977) qualitatively

observed sand transport as ‘nil,’ ‘light,’ or ‘strong.’ They compared these visual observations to the anemometer readings and estimated threshold shear velocity. They used erosion pins (wooden rulers) to measure deposition on the slipfaces of five barchan dunes having a mean grain diameter of 0.17 mm.

2.2 Performance of the Models in Previous Studies

A gap has typically been observed between measured and predicted transport rates. Usually, predicted transport rates are larger than measured rates. Sherman et al. (1998) found that the Zingg (1953) model produced a much better result than the other models, but still only explained about 40% of the variance in the rates of transport. Sherman and Li reevaluated the aeolian transport in 2011 using the same data and followed several quality control criteria and concluded that the Bagnold (1936) model presents the best compatibility between the observed and predicted transport rates. The models of Kadib (1965) and Hsu (1971) came in second place in their study. Sherman and Li (2011) indicated that the models of Lettau and Lettau (1977) and Kawamura (1951) display the poorest performance. Berg (1983) found the model of Kadib (1965) model as the most prominent in predicting transport rate. Sarre (1988) found Kawamura (1951) model to provide the best fit to measurements collected in the intertidal zone. Svasek and Terwindt (1974) also found that the model of Kawamura (1951) provided the best representation of their field data. Berg (1983) and Sarre (1988) found the model of Lettau and Lettau (1977) to be estimated well within the intertidal zone. Each model performs differently in each experimental condition. Overall, there is no clear consensus regarding which model(s) provide the most accurate predictions.

2.3 Site Specific Complications

The models described above were all developed based on consideration of ideal conditions, a flat, uniform, dry, unvegetated sediment bed. Under such conditions, aeolian transport rates would depend only on wind speed and sediment size. However, in natural environments there are many site-specific factors that depart from the ideal and complicate the process. Major factors include cohesion induced by moisture (Belly 1964, Cornelis and Gabriels 2003, McKenna-Neuman and Nickling 1989, Namikas and Sherman 1995), local slope effects (Hesp et al. 2005, Iversen and Rasmussen 1999, White and Tsoar 1998), the fetch effect (Davidson-Arnott and Bauer 2009, Schönfeldt 2004, Stout and Zobeck 1997, Wiggs et al. 2004), and the presence of vegetation (Arens et al. 2001, Bauer et al. 2009, Hesp 1981, Kuriyama et al. 2005, Lancaster and Baas 1998, Niedoroda et al. 1991).

It has long been recognized that moisture content is an important control on aeolian sediment transport (Belly 1964, Nickling and Davidson-Arnott 1990, Namikas and Sherman 1995, Cornelis and Gabriels 2003, Cornelis et al. 2004, Ravi et al. 2006). Although a number of models of moisture effects have been developed, modeling of aeolian transport is further hampered by complex spatial and temporal variations in surface moisture content especially in coastal environments (Jackson and Nordstrom 1997, Atherton et al. 2001, Wiggs et al. 2004a, Yang and Davidson-Arnott 2005). In practice, interstitial moisture increases the threshold of motion and consequently reduces the rate of transport compared to dry conditions (Cornelis and Gabriels 2003, Wiggs et al. 2004b, Davidson-Arnott et al. 2005, McKenna Neuman and Langston 2006). Numerous models have been proposed to represent the influence of moisture on the threshold of motion (Namikas and Sherman 1995, Cornelis and Gabriels, 2003) but their predictions differ by an even larger degree than those of the ideal transport models under considerations here.

The effects of slope on aeolian transport are important on the surfaces of beaches, sand sheets and dunes (Iversen and Rasmussen 1999). Most aeolian transport takes place on windward slopes. Windward slopes on barchan or transverse dunes are typically of the order of 10° to 12° (Lettau and Lettau 1976, Haff and Presti 1995, Mulligan 1988). In aeolian environments with seasonal changes in wind direction, temporary inclinations of 30° or more may be found on the windward slopes of seif dunes, reversing dunes or star dunes (McKee 1966, Tsoar 1983). On negative slopes where steepness is less than the angle-of-repose, aeolian transport is usually transitional, associated with seasonal changes in wind direction. In coastal environments, wave erosion can produce temporary slopes on the seaward slopes of foredunes that approach vertical, effectively preventing landward transport.

The 'fetch effect' refers to a progressive increase in sediment transport rates with downwind distance from a zone of no transport, such as a paved surface, the leading edge of a sand sheet, or a saturated coastal foreshore. Moving inland from a shoreline Bauer et al. (2009) found that an internal atmospheric boundary layer developed with a steep vertical gradient that implies large shear stress and indicates large potential to entrain and transport sediment. Therefore, aeolian transport models would suggest that the greatest rates of transport should occur on the foreshore and decrease in the downwind direction. However, because the saltation system is not able to respond immediately to this large capacity and no sediment is being initiated from upwind, Bauer et al. (2009) found that the rate of aeolian sediment transport on the foreshore is typically much smaller than predicted on the basis of shear stress alone. The saltation system needs to develop over a downwind distance before achieving maximum rates of transport. The wind-parallel length of this zone of adjustment, measured from the leading edge of the sand surface, is termed the 'fetch distance' (Bauer and Davidson-Arnott 2009).

Vegetation acts as a roughness element that inhibits wind flow and reduces the near-bed wind velocity. Laboratory and field experiments have confirmed that vegetation decreases sediment movement and induces accumulation (Woodhouse 1978, Niedoroda et al.1991, Wolfe and Nickling 1993, Kuriyama et al. 2005). As yet vegetation has not been directly incorporated into models of the transport rate in a generally applicable fashion.

2.4 Mass-weighted Frequency Distribution

The sorting of sediments is known to have an impact on sediment transport (Davidson-Arnott and Bauer 2009, Grass 1971, Logie 1981, Neuman 2003, Nickling 1988). It has been noted that the performance of transport models tends to decrease as sediment becomes more poorly sorted (Horikawa et al. 1986). This problem may derive from the common approach to representing the sediment bed in terms of characteristic mean grain diameter based on the grain axes dimensions. Edwards and Namikas (2015) developed a mass-weighted size distribution of the sediment population to more closely approximate the actual resistance to motion of the particles. The grain diameter that corresponds to the mean of the mass-weighted distribution (d_r) is given by:

$$d_r = 2 * \sqrt[3]{\frac{3}{4\pi} * \frac{\sum (f*V)}{100}} \quad \text{..... (14).}$$

where f is the frequency (%) of each size class, and V is the volume of the midpoint grain for each size class. Edwards and Namikas (2015) implemented this approach to model threshold shear velocities and found that it provides a substantial improvement in predictive capability for available laboratory data. This study uses the mass-weighted grain diameter from Equation 14 to determine whether the application of the mass-weighted approach will improve prediction of aeolian transport rates.

To understand the effect of sorting, consider four-grain size distributions with sorting values of 0.2, 0.4, 0.6, and 0.8, respectively, and all characterized by a mean diameter of 0.25 mm (Figure 3). To approximate the weight force resisting motion in these grain size distributions, the midpoint diameter of each size class is used to calculate the mass of a grain representative of that size class. The mass-weighted diameter becomes increasingly large as the sorting value increases. For the sediments in Figure 3, transformation from d_{50} to d_r correspond to an increase in the representative diameter of 0.014, 0.064, 0.17, and 0.38 mm, respectively.

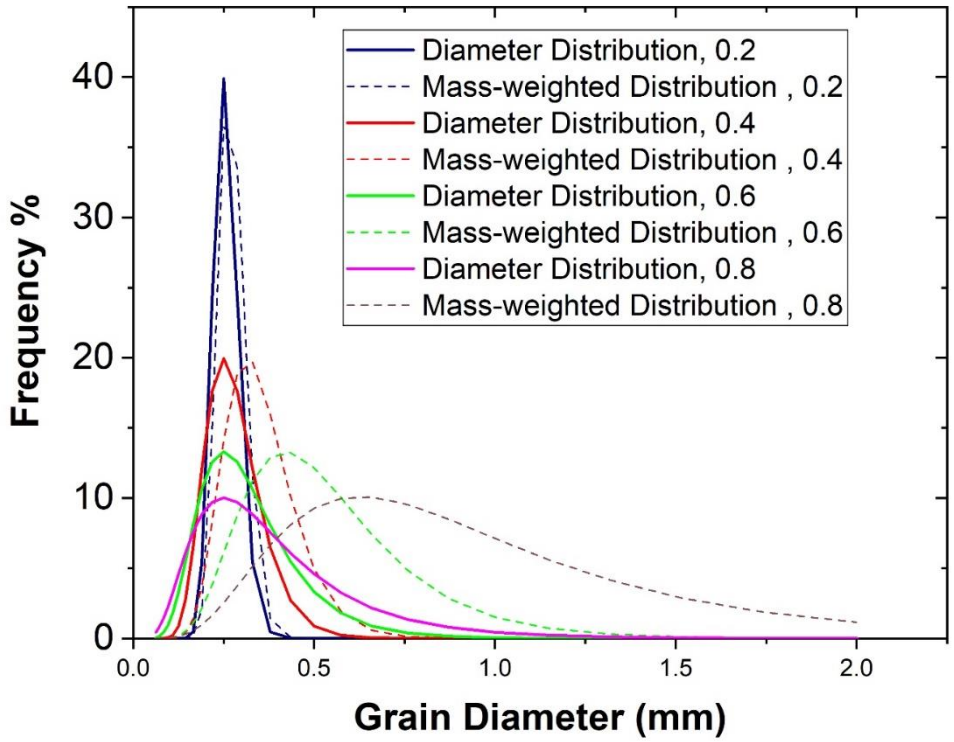

Figure 3: Transformations of grain size distributions with mean of d50 = 0.25 mm and a range of sorting values (0.2, 0.4, 0.6, and 0.8) to mass-weighted frequency distributions of resistance to motion, with means of dr = 0.26, 0.31, 0.42, and 0.63 mm.

It is evident that if grain size distributions are weighted by grain mass, an increase in the range of sizes present in the sediment bed can have a substantive effect on the expected resistance to motion (Edwards and Namikas 2015).

2.5 Apparent von Kármán's Parameter

Shear velocity (u_*) is usually estimated from measured velocity profiles as:

$$u_* = km \quad \ldots\ldots\ldots\ldots\ldots\ldots\ldots\ldots\ldots\ldots\ldots\ldots\ldots\ldots\ldots\ldots\ldots\ldots\ldots\ldots \quad (15).$$

where k is the von Kármán constant (typically it is assumed that k = 0.4), and m is the slope of the near-surface velocity profile in logarithmic space. However, Li et al. (2010) found that as the sediment transport rate Q increases, the value of the von Kármán parameter as determined from best-fits to field data tends to decrease. Li et al. (2010) proposed an apparent von Kármán constant (k_a) that is defined as:

$$k_a = -3.03Q + 0.40 \quad \ldots\ldots\ldots\ldots\ldots\ldots\ldots\ldots\ldots\ldots\ldots\ldots\ldots\ldots\ldots\ldots\ldots\ldots\ldots\ldots \quad (16).$$

where Q is the sediment transport rate. Li et al. (2010) established the above relationship for transport rates ranging from 0.015 to 0.0315 $kgm^{-1}s^{-1}$. However, larger transport rates will generate very small or even negative values of k_a. In practice the value of k_a must be positive. Therefore, the true relationship between Q and k_a cannot be linear as expressed in Equation 16. Li et al. (2010) concluded that Equation 16 is not universally applicable. Therefore, given a wide range of transport rates this approach might show poor agreement between measured and predicted rates. With very large rates of transport the result would be poorer than the standard approach of assuming the von Kármán parameter to be constant.

2.6 Available Data

To apply these models, three variables are required. These are measurements of the transport rate, shear velocity, and the sediment size frequency distribution. Previous studies that provide all of the required variables include Belly (1962), Kadib (1963), Kadib (1965), Kubota et

al. (1982), Berg (1983), Butterfield (1991), Namikas (2003) and Huang et al. (2010). In a number of other studies transport and shear velocity data are provided, but the sediment size frequency distribution is not reported (Bagnold 1941, Kawamura 1951, and Sherman et al. 1998). In this latter case, the frequency distribution can be estimated if both the mean grain size and sorting coefficient are provided. This is accomplished by inputting those values into a lognormal probability density function. It is noted that this adjustment adds an additional element of uncertainty so that these datasets are treated separately.

A total of six laboratories and three field studies were identified that provide all required variables. These include the laboratory studies of Belly (1962), Kadib (1963), Kadib (1965), Kubota et al. (1982), Butterfield (1991), and Huang et al. (2010), and the field studies of Berg (1983), Butterfield (1991) and Namikas (2003).. Key details of these studies are provided in Table 1.

Table 1: Summary of datasets with reported frequency distributions

Study	Location	No. of Runs	d_{50} (mm)	u_* (ms^{-1})	Q_{min}	Q_{max}
					$kgm^{-1}s^{-1}$	
Belly (1962)	Laboratory	18	0.24-0.48	0.30-0.64	0.0012	0.11
Kadib (1963)	Laboratory	14	0.145	0.22-0.84	0.0001	0.093
Kadib (1965)	Laboratory	20	0.88-1.00	0.37-1.07	0.0215	0.674
Kubota et al. (1982)	Yonezu Beach, Japan	26	0.24-0.47	0.22-0.54	0.0002	0.025
Berg (1983)	Dillon Beach, England	12	0.26-0.38	0.37-0.51	0.0112	0.08
Butterfield (1991)	Laboratory	38	0.177	0.48-1.05	0.018	0.045
Butterfield (1991)	Bordeira, Portugal	25	0.27	0.45-0.85	0.015	0.055
Namikas (2003)	Oceano Beach, CA	9	0.25	0.27-0.63	0.0008	0.029
Huang et al. (2010)	Laboratory	4	0.228	0.32-0.85	0.0022	0.065

Collectively, they provide 166 transport rate measurements that range from 0.0001 to 0.674 $kgm^{-1}s^{-1}$. They include a wide range of mean sediment sizes from 0.145 to 1.00 mm, and of shear velocities which range from 0.22 to 1.07 ms^{-1}. The measured transport rates are plotted as a function of shear velocity in Figure 4. The variety of sites and the mix of field and laboratory data, together with the wide range of wind and transport intensities, should provide for a rigorous test of the modeling approaches.

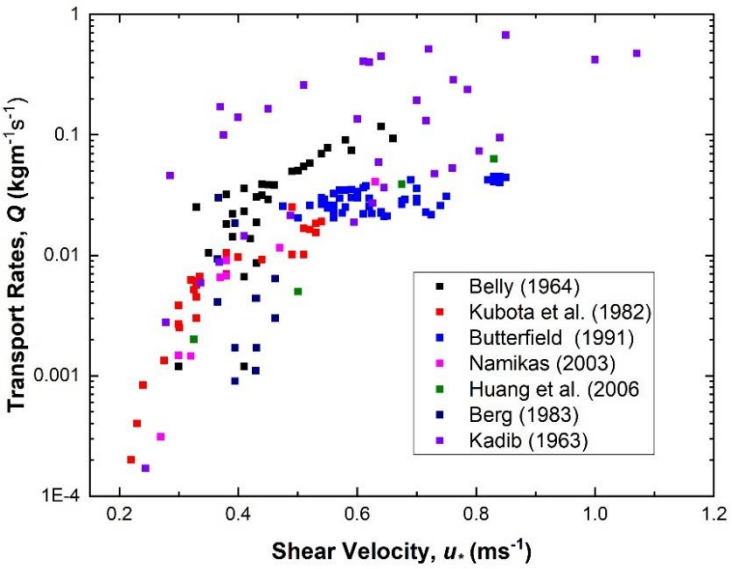

Figure 4: Measured transport rates as a function of shear velocity for reported frequency datasets.

An additional three studies that lack frequency distributions but do provide sediment mean and sorting values were identified. Key details of these studies are summarized in Table 2. The measured transport rates are shown in Figure 5. Two of the studies were conducted in laboratory wind tunnels (Bagnold 1936, Kawamura 1951) and one was conducted at a field location (Sherman et al. 1998). Collectively, these studies provide an additional 70 transport rate measurements that range from 0.00001 to 0.430 $kgm^{-1}s^{-1}$. They include a range of mean sediment size from 0.17 to 0.30 mm, and the measured shear velocities range from 0.23 to 1.09 ms^{-1}.

Table 2: Summary of datasets with estimated frequency distributions

Study	Location	No. of Runs	d_{50} (mm)	u_* (ms^{-1})	Q_{min}	Q_{max}
					$kgm^{-1}s^{-1}$	
Bagnold (1941)	Laboratory	6	0.18-0.30	0.25-0.88	0.0029	0.122
Kawamura (1951)	Laboratory	13	0.21	0.27-1.09	0.001	0.430
Sherman et al. (1998)	Inch Spit	51	0.17	0.23-0.65	0.00001	0.0222

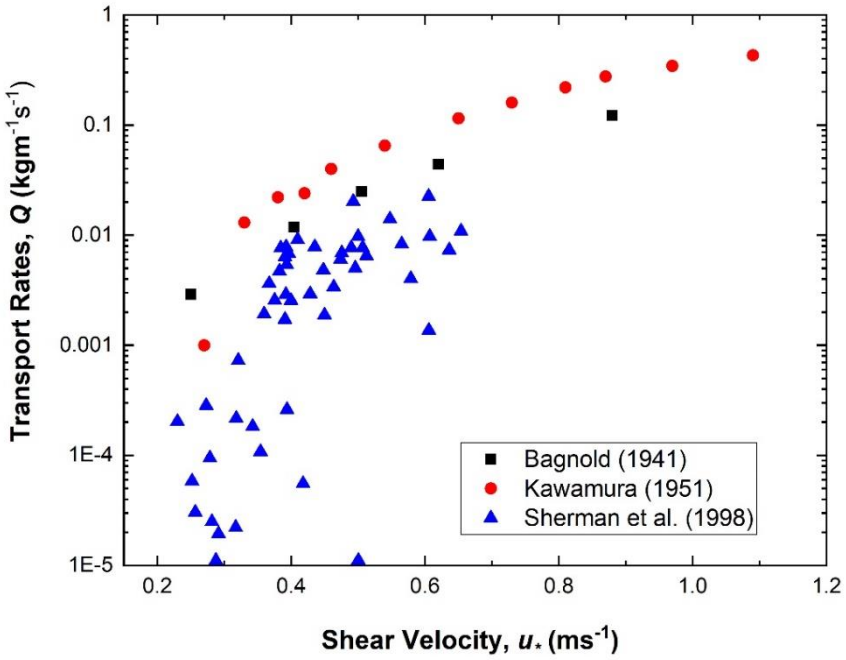

Figure 5: Comparison of transport rates of estimated frequency datasets in each shear velocity.

2.7 Descriptions of the Experiments

A brief overview of the experiments that generated the data used herein is presented below, for comparison and evaluation. Details of the experiments for the data reported in Bagnold (1941), Kawamura (1951) and Kadib (1965) are described in section 2.1 of this chapter. The remainder of the studies are described below.

2.7.1 Belly (1962).

This experiment was conducted in a wind tunnel located at the Richmond Field Station of the University of California. The tunnel was 1.23 m wide, 0.76 m high, and 30.48 m long, and was

made of plywood. The wind was generated by a fan installed at the exit end. A standard Prandtl type pitot was used to measure the wind velocities, which ranged from 7.31 to 12 ms^{-1}. A vertical trap designed by Horikawa and Shen (1960) was placed at the middle of the tunnel. A horizontal trap was fixed at the end of the sand bed. The run durations ranged from 5 to 30 minutes. The grain size varied from 0.24 to 0.48 mm and the resulting transport rates ranged from 0.0012 to 0.11 $kgm^{-1}s^{-1}$.

2.7.2 Kubota et al. (1982)

This field study was carried out on Yonezu Beach which is situated at the middle of the main island of Japan. Beach sediments ranged in size from 0.1 to 0.8 mm, with a median diameter of 0.4 mm. An anemometer array comprised of six ultrasonic anemometers was used to quantify the wind speed. The lowest height used for the wind speed was 10 cm. Kubota et al. (1982) used two different traps for the measurement of transport rates. The first was a conventional total quantity-type trap and the other was a trench trap. Each sampling period was 10 minutes. The measured shear velocities varied from 0.22 to 0.54 ms^{-1} and the resulting transport rates ranged from 0.00022 to 0.025 $kgm^{-1}s^{-1}$.

2.7.3 Berg (1983)

Berg (1983) conducted several pilot studies to refine the experimental procedure. The study site was a near-horizontal sand surface on a dune crest at the coastal dune complex near Dillon Beach, California. Berg (1983) used fluorescent tracer techniques originally applied in fluvial environments (e.g. Crickmore and Lean 1962, Crickmore 1967) to measure aeolian transport rates. Three different commercial sands (Del Monte White Sand 30 Mesh, Lone Star Lapis Lustre#20, and Pacific Cement and Aggregates Lapis Lustre # 2) were used as tracer sands. Wind speed was

measured using two ‘freeze’ type anemometers made by Belfort Instrument Company. Anemometer recording was made at 10-minute intervals throughout the experiment. The measured shear velocities varied from 0.37 to 0.51 ms^{-1} and the resulting transport rates ranged from 0.0112 to 0.08 $kgm^{-1}s^{-1}$.

2.7.4 Butterfield (1991)

Butterfield (1991) conducted both natural field and portable wind tunnel experiments to measure wind blown sand transport rates. He considered both steady (wind tunnel) and unsteady (natural) wind flow in field conditions. The wind field was measured using robust hot-wire anemometers and naturally ventilated, wedge-shaped sand trap fitted with a sensitive load cell was used to measure transport rates. Field experiments took place on interdune and intertidal sands at Ynyslas, Wales, and in the crestal regions of transverse coastal dunes at Praia Bordeira, South West Portugal. Use of the portable wind tunnel allowed controlled variation of the airflow and represented a major advance in field measurement of aeolian sand transport.

2.7.5 Sherman et al. (1998)

Sherman et al. (1998) conducted a field experiment at Inch Spit located on the southwestern coast of the Republic of Ireland. The site was a gently sloping intertidal zone and beach berm. Wind speed was measured using three-cup anemometers. Five anemometer arrays were deployed, each composed of four anemometers at elevations of 0.25, 0.50, 0.75 and 1.00 m. Relative anemometer accuracy was evaluated by an in-situ cross calibration process. Anemometers were sampled at 1s intervals for 17.1 m periods, and total transport at each array location was measured using Leatherman-type traps. Sediment samples from both the traps and from several sub-environments were subjected to grain size analyses and found to be almost uniform.

2.7.6 Namikas (2003)

Namikas (2003) conducted field experiments in the Oceano Dunes State Vehicular Recreation Area (SVRA) on the central California coast. A broad, relatively flat and unvegetated beach berm was selected for the study, which extended inland from the berm crest for a distance of about 250 m. The slope from the berm crest to the instrument array was less than 1 degree. The average grain size of the study area was 0.25 mm with a sorting value of 0.37. Eight rotating-cup anemometers were used to monitor the vertical wind speed. A wind vane was placed at the top of the mast to monitor direction. The vertical distribution of the horizontal mass flux was quantified by installing a set of 15 wedge-shaped sediment collectors called VTRAP. The horizontal distribution of the vertical mass flux was measured using a 2.1 m long trough-type trap which was subdivided into 35 compartments.

2.7.7 Huang et al. (2010)

Huang et al. (2010) conducted experiments in the wind tunnel at the Institute of Cold and Arid Region Environmental Engineering of the Chinese Academy of Sciences. The wind tunnel floor was covered with a 0.1 m thick layer of mixed sand. The sediment had a mean grain diameter of 0.228 mm and was collected from a sand dune at the southeastern edge of the Tengger Desert. Wind speed was measured using an array of 10 pitot static probes mounted at heights of 0.003, 0.006, 0.01, 0.015, 0.03, 0.06, 0.12, 0.2, 0.35, and 0.5 m above the sand bed. Experiments at each wind speed were repeated three times to improve accuracy.

CHAPTER 3: METHODOLOGY

The goal of this study is to evaluate the utility of two new approaches to modeling aeolian transport rates. To make the study as robust as possible, it employs a very large dataset of transport rate measurements drawn from the literature. A total of twelve suitable datasets have been identified, which collectively provide 227 measurements of aeolian transport rates involving a wide range of experimental conditions from both laboratory and field studies. The study employs a set of seven transport rate models, which include the most commonly used approaches.

3.1 Treatment of Empirical Coefficients

The Bagnold (1937), Kawamura (1951), Zingg (1953), Owen (1964), Hsu (1971), and Lettau and Lettau (1977) models all have empirical coefficient that scale the predicted transport rates (Table 3). This study tested the empirical coefficient values determined in the original studies, as well as those found in later studies through best-fit methods. New best-fit coefficients were also determined for the modified models using regression analysis, with the exception of Owen (1964) and Hsu (1971). To obtain the new empirical coefficients, the least square regression lines for observed versus predicted transport rates were forced through zero and the resulting slope was used as the correction factor.

Table 3: Empirical coefficient for different models

Model	Empirical coefficient Range	Original value
Bagnold (1936)	1.5-3.5	1.8
Kawamura (1951)	1-2.78	2.78
Zingg (1953)	0.83	0.83
Owen (1964)	Fall velocity, w_s	From Chen and Fryrear (2001) (Eq. 6)
Kadib (1965)	Φ, Transport Intensity	From the graphical method (Eq. 8)
Hsu (1971)	Best fitted line	From best-fitted line (Eq. 11)
Lettau (1977)	4.7-9.9	4.2

The new empirical coefficients were calculated by dividing the original coefficients by the correction factor. The models of Owen (1964) and Hsu (1971) have their original coefficient from the correction factor obtained by regression. Recalibration of above two models will bring additional complexity to the process. Therefore, both of these models were excluded from the recalibration process.

3.2 Conversion of Mean Diameter to the Mean of Mass-Weighted Frequency Distribution

To implement the mass-weighted frequency distribution of sediment population, mean grain diameter d_{50} was transformed to the mean of the mass-weighted frequency distribution d_r following Equation 14. The original and converted mean grain sizes are given in Table 4. For studies that did not report the complete frequency distribution, the distribution was estimated from sorting values using a probability density function. The estimated mass-weighted mean grain sizes resulting from the latter approach are given in Table 5.

Table 4: Mass-weighted mean grain size from reported frequency distributions

Study	d_{50} (mm)	d_r (mm)
Belly (1962)	0.44	0.46
Belly (1962)	0.30	0.34
Kadib (1965) Sand D	1.00	1.05
Kadib (1965) Sand E	0.88	0.99
Kadib (1963) Sand C	0.14	0.16
Kubota et al. (1982) Sand A	0.27	0.30
Kubota et al. (1982) Sand B	0.26	0.29
Kubota et al. (1982) Sand C	0.30	0.32
Berg (1983) Tracer Sand 1	0.26	0.31
Berg (1983) Tracer Sand 2	0.65	0.69
Berg (1983) Tracer Sand 3	0.99	1.04
Butterfield (1991) Wind Tunnel	0.17	0.20
Butterfield (1991) Field	0.27	0.29
Namikas (2003)	0.25	0.29
Huang et al. (2006)	0.22	0.26

Table 5: Mass-weighted mean grain size from estimated frequency distributions

Name of the Study	d_{50}	Sorting	d_r
Bagnold (1941)	0.24	0.06	0.247
Kawamura (1951)	0.21	0.65	0.270
Sherman et al. (1998)	0.17	0.38	0.204

3.3 Efficiency of Probability Density Function (PDF) to Estimate Frequency Distribution

To evaluate the accuracy of using a probability density function to estimate the sediment frequency distribution, the technique was used to estimate mass-weighted means for the six studies that reported both full sediment frequency distributions and sorting coefficients (Table 6).

Table 6: Comparision of the mass-weighted mean from estimated and reported frequency.

Study	Mean Diameter, d_{50} (mm)	Sorting (Phi)	d_r from reported frequency (mm)	d_r from estimated frequency using PDF (mm)
Kadib (1965) sand D	1.00	0.29	1.05	1.12
Kadib (1965) sand E	0.88	0.30	0.99	1.00
Berg (1983) tracer sand 1	0.26	0.64	0.31	0.47
Berg (1983) tracer sand 2	0.65	0.32	0.69	0.75
Berg (1983) tracer sand 3	0.99	0.33	1.04	1.15
Namikas (2003)	0.25	0.37	0.29	0.30

The frequency distributions estimated from probability density function (PDF) do show some differences from the reported frequency distribution. The mass-weighted means determined from estimated distributions are consistently somewhat larger than those determined from the reported frequency distributions (Table 6.). Despite this systematic difference, regression analysis indicates that the mean diameters determined by the two approaches are in reasonable agreement, with an R^2 value of 0.973 and root mean square error (RMSE) of only 0.06. This finding demonstrates that the probability density estimates provide a reasonable approximation of the mass-weighted means determined from reported frequency distributions.

3.4 Use of Apparent von Kármán parameter to Calculate Shear Velocity

Where appropriate reported shear velocities were recalculated using the apparent von Kármán parameter, following Equation 16 (Li et al. 2010). Li et al. (2010) found this approach to be effective for transport rates ranging from 0.0150 to 0.0315 $kgm^{-1}s^{-1}$. However, transport rates employed in this study cover a much wider range (0.00001 to 0.430 $kgm^{-1}s^{-1)}$. The value of apparent von Kármán parameter becomes increasingly small with larger transport rates, and is negative for transport rates larger than 0.13 $kgm^{-1}s^{-1}$, which is clearly an unrealistic result Therefore, observations of transport rates greater than 0.0315 $kgm^{-1}s^{-1}$ were not included in this portion of the analysis.

CHAPTER 4. RESULTS AND DISCUSSION

This chapter presents the results and analyses of the two modified approaches to aeolian transport modeling. Results of the study are grouped as a comparison of predictions obtained with mean diameter (d_{50}) and mass-weighted mean (d_r) with original von Kármán constant (k), and then a comparison of those two with inclusion of the apparent von Kármán parameter (k_a) in appropriate cases. These comparisons employ the original empirical coefficients for each model. Finally, results with recalibrated empirical coefficients (both with and without d_r and k_a) are presented.

4.1 Comparative Results of d_{50} and d_r with Original von Kármán Constant (k=0.4)

4.1.1 Reported frequency datasets

After converting reported mean grain diameters (d_{50}) to mass-weighted means (d_r), regression analyses were performed. This was done separately for datasets with a reported frequency distribution and those for which it was estimated. The statistical results for the reported frequency datasets are summarized in Table 7. To identify the statistical improvement associated with d_r, one-way ANOVA was performed and corresponding p values are summarized in Table 7. Values greater than 0.05 indicates a significant difference between the fit obtained using d_{50} and d_r, and p values less than 0.05 indicate no significant difference between the two approaches.

Table 7: Results of regression analysis for reported frequency datasets with original (d_{50}) and converted mean diameter (d_r) and k=0.4

Results from d_{50} and k =0.4 (Reported frequency datasets)								
Models	Bagnold	Kawamura	Zingg	Owen	Lettau	Hsu	Kadib	Average
R^2	0.521	0.222	0.571	0.476	0.368	0.485	0.285	0.418
RMSE	0.044	0.067	0.026	0.017	0.078	0.09	0.007	0.047
a	0.027	0.059	0.01	0.014	0.042	0.018	0.011	0.026
b	0.470	0.364	0.311	0.163	0.610	0.892	0.48	0.470

(Table 7 continued)

Results from d_r and k = 0.4 (Reported frequency datasets)								
Models	Bagnold	Kawamura	Zingg	Owen	Lettau	Hsu	Kadib	Average
R^2	0.531	0.226	0.595	0.483	0.368	0.564	0.311	0.439
RMSE	0.045	0.067	0.027	0.017	0.08	0.101	0.008	0.049
a	0.028	0.059	0.012	0.016	0.045	0.012	0.012	0.026
b	0.482	0.370	0.333	0.168	0.615	0.910	0.500	0.481
Change in R^2	0.010	0.004	0.024	0.007	0.000	0.079	0.026	0.021
Change in RMSE	0.001	0.000	0.001	0.000	0.002	0.011	0.001	0.002
P value	0.091	0.000	0.115	0.082	0.000	0.391	0.421	

All models other than Kawamura (1951) and Lettau and Lettau (1977) show some degree of increase in the agreement between observed and predicted rates of aeolian sediment transport. The increase is small but statistically significant for Bagnold (1936), Zingg (1953), Owen (1964), Hsu (1971) and Kadib (1965). The average increase in the level of explanation is about 5% (a 2.1% absolute increase from the original 41.8% is a 5% increase over the original predictive capability). This is relatively small, but does represent a modest improvement in predictive capabilities. The largest increase in R^2 value occurs with the Hsu (1971) model (0.485 to 0.564) with about a 16% improvement in the level of explanation. The R^2 value for the Zingg (1953) model increases from 0.57 to 0.59, while R^2 values increase only slightly for the models of Owen (1964) and Bagnold (1936). The RMSE values similar or increase slightly compared to those from d_{50}. The slope (b) and intercept (a) of the regression analyses are mentioned in the Table to define the regression equation. These parameters help to define the range of the prediction of the aeolian transport models.

For datasets with estimated frequency distributions the regression results are summarized in Table 8. The statistical significance of the predictive improvement associated with the use of d_r is again determined from the p value of the one-way ANOVAs. These datasets included a much

smaller range in grain size (d_{50}: 0.17 - 0.30 mm) and provided better predictive fits than the more variable grain-size datasets with reported frequency distributions.

Table 8: Comparison of the results of regression analysis for estimated frequency datasets with original (d_{50}) and converted mean diameter (d_r) and k=0.4.

Results from d_{50} and k=0.4 (Estimated frequency)								
Models	Bagnold	Kawamura	Zingg	Owen	Lettau	Hsu	Kadib	Average
R^2	0.891	0.881	0.892	0.862	0.895	0.869	0.643	0.848
RMSE	0.015	0.030	0.007	0.007	0.028	0.015	0.004	0.015
a	0.013	0.028	0.005	0.008	0.017	0.015	0.009	0.014
b	0.537	1.020	0.239	0.210	1.037	0.479	0.074	0.514
Results from d_r and k=0.4 (Estimated frequency)								
R^2	0.908	0.918	0.892	0.880	0.905	0.867	0.690	0.866
RMSE	0.015	0.027	0.007	0.007	0.029	0.014	0.005	0.015
a	0.014	0.006	0.005	0.009	0.017	0.013	0.009	0.011
b	0.607	0.287	0.239	0.235	1.139	0.445	0.086	0.434
Change in R^2	0.017	0.037	0.000	0.018	0.010	-0.002	0.047	0.018
Change in RMSE	0.000	-0.023	0.000	0.000	0.001	-0.001	0.001	-0.003
P value	0.061	0.154	0.000	0.124	0.099	0.003	0.331	

Use of the mass-weighted mean diameter produces an improvement in R^2 value for 5 of the seven models. The improvement is statistically significant for Bagnold (1936), Kawamura (1951), Owen (1964), Lettau and Lettau (1977), and Kadib (1965). The greatest improvement occurs with the Kadib (1965) model (0.64 to 0.69). The Kawamura (1951) model exhibits an increase in R^2 from 0.881 to 0.918 and the RMSE value decreases from 0.030 to 0.027. The Kawamura (1951) model not only shows improvement in statistical agreement but also provides the highest R^2 value among all models for d_r. The R^2 value slightly increases for the models of Bagnold (1936), Owen (1964), and Lettau and Lettau (1977). The average R^2 value for all models increases from 0.848 to 0.866 and RMSE value remains approximately identical with use of the mass-weighted diameter.

Broadly, the predictive capability of the models was quite different for the reported frequency and estimated frequency datasets. The reported frequency datasets include a wider range of transport rates (0.0001 to 0.674 $kgm^{-1}s^{-1}$) and many more individual observations drawn from a larger number of studies. All of these factors potentially enhance observation errors, and the predictive capability of the models for these data was moderate. The estimated frequency datasets contained a comparatively small range of transport rates (0.0001 to 0.43 $kgm^{-1}s^{-1}$), and fewer individual observations drawn from a small number of studies. This reduces the potential for errors and inconsistency, and generated a higher level of predictive capability.

Statistically significant improvements for both reported and estimated frequency datasets are observed in Owen (1964) and Kadib (1965) model. The model of Kawamura (1971) and Lettau and Lettau (1977) performed poorly for reported frequency datasets. However, for estimated frequency datasets, no significant improvement is observed for Bagnold (1936), Zingg (1953), and Hsu (1971) models. For the reported frequency datasets, the greatest improvement in goodness of fit parameters are observed in the Hsu (1971) and Kadib (1965) models. However, for the estimated frequency datasets, the greatest improvements are observed in Kadib (1965) and Kawamura (1951) model. Therefore, Kadib (1965) model shows the largest improvement for both datasets and proves its effectiveness to the application of mass-weighted mean for wide range of data characteristics. It can be concluded that the impact of the modification of mean diameter varies model to model and seems to depend largely on the data characteristics (transport rates, grain size and shear velocity ranges).

Predictive capability obtained through the use of d_r can be seen in Figure 6. All of the models tend to overpredict at lower transport rates and underpredict the highest rates. There are several observed transport rates greater than 0.1 $kgm^{-1}s^{-1}$ and Kawamura (1951), Owen (1965),

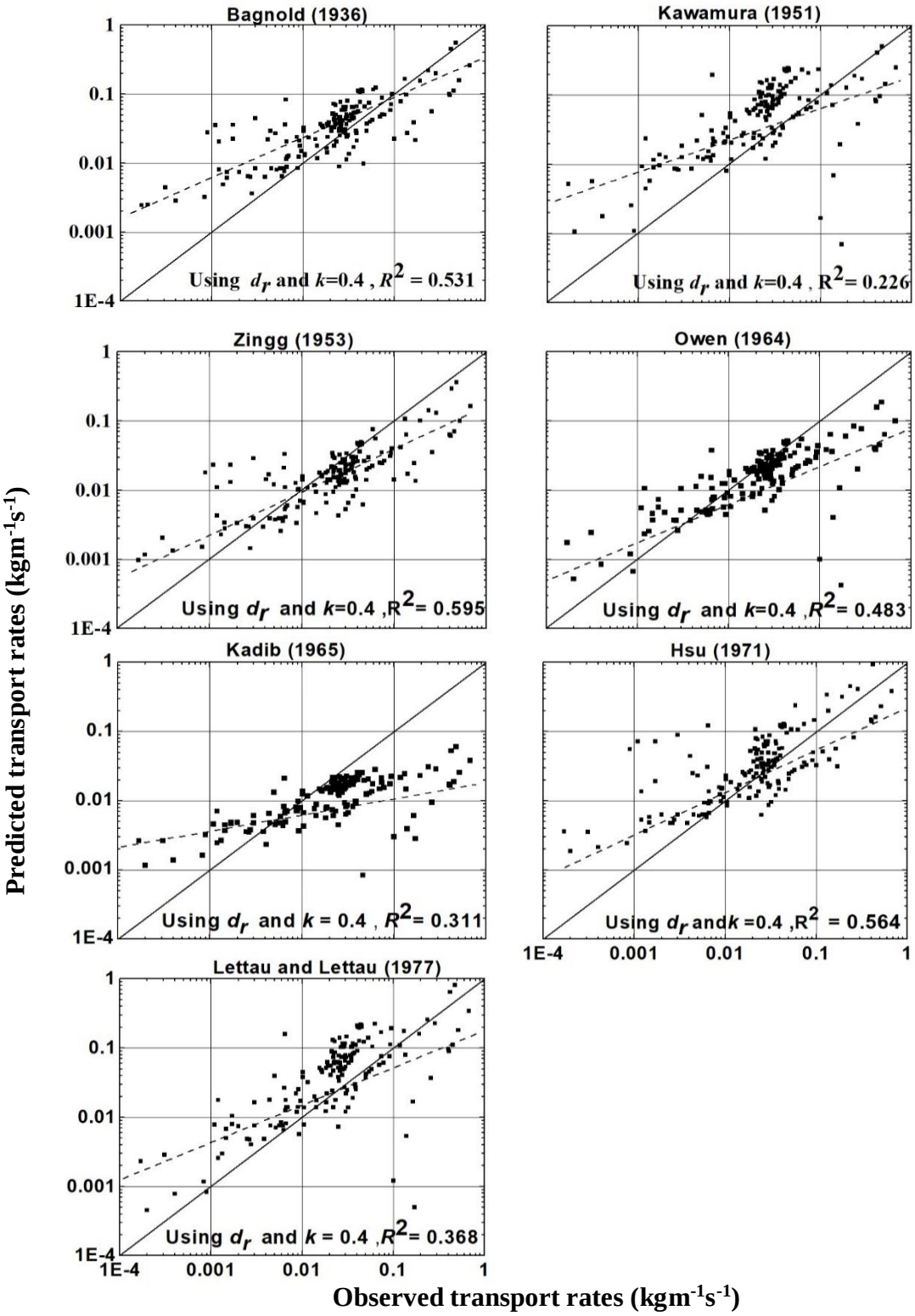

Figure 6: Comparison of observed and predicted rates after corrections for mean diameter of reported frequency datasets. Dashed line is best-fit from linear regression, solid line is a one-to one relation.

Kadib (1965) and Lettau and Lettau (1977) models clearly perform poorly at these transport rates. However, the models of Hsu (1971), Zingg (1953), and Bagnold (1936) provide a more reasonable representation. Therefore, the observations greater than 0.1 $kgm^{-1}s^{-1}$ are likely disproportionately responsible for providing poor results in the regression analyses. The models of Bagnold (1936), Zingg (1953) and Hsu (1971) perform best visually in addressing the larger transport rates and also provide better agreement in terms of statistical goodness of fits.

Several models are found to be sensitive to the change of mean diameter. The use of d_r is found to be the most effective for the Hsu (1971) model for the reported frequency datasets containing wide range of grain sizes, and Kadib (1965) model for the estimated frequency datasets containing small range of grain size. Transport rates greater than 0.1 $kgm^{-1}s^{-1}$ are found responsible for providing poor results in the regression analyses. Therefore, the impact of the mean of the mass-weighted frequency distribution is apparent. Improvement of predictive capability from this approach varies between models and depends on the data characteristics (transport rates, grain size and shear velocity ranges).

4.1.2 Comparison of Wind Tunnel and Field Data

In the next section the wind tunnel datasets and field datasets are examined independently to identify the influence of the different experimental approaches. There are seven wind tunnel experiments containing 113 transport rate observations. Results of the transformation of mean grain diameter are summarized in Table 9 and scatter distributions are shown in Figure 7.

Table 9: Comparison of the results of regression analysis of wind tunnel data with original (d_{50}) and converted mean diameter (d_r) and k=0.4.

Results from d_{50} and k =0.4 (Wind Tunnel)								
Models	Bagnold	Kawamura	Zingg	Owen	Lettau	Hsu	Kadib	Avg.
R^2	0.531	0.368	0.552	0.498	0.402	0.438	0.383	0.453
RMSE	0.053	0.085	0.0315	0.02	0.094	0.113	0.008	0.058
a	0.031	0.073	0.011	0.017	0.052	0.025	0.013	0.032
b	0.453	0.41	0.29	0.158	0.615	0.795	0.044	0.395
Results from d_r and k =0.4 (Wind Tunnel)								
R^2	0.548	0.361	0.583	0.499	0.401	0.492	0.393	0.468
RMSE	0.053	0.136	0.085	0.021	0.119	0.126	0.009	0.079
a	0.031	0.112	0.03	0.017	0.063	0.013	0.013	0.04
b	0.485	0.675	0.828	0.165	0.796	1.023	0.046	0.574
Change in R^2	0.017	-0.007	0.031	0.001	-0.001	0.054	0.01	0.015
Change in RMSE	0.00	0.051	0.0535	0.001	0.025	0.013	0.001	0.021
P value	0.001	0.000	0.081	0.002	0.000	0.254	0.061	

Only three of the seven models show a statistically significant improvement. The most significant improvements occur with the Zingg (1953) and Hsu (1971) models. The Zingg model shows an increase in R^2 from 0.552 to 0.583, and for Hsu (1971) the improvement is from 0.438 to 0.492. There observe almost identical results in all models other than Zingg (1953) and Hsu (1971). All the models other than Bagnold (1936) indicate an increased RMSE value after the transformation.

The scatter distributions of observed and predicted rates are summarized in Figure 7. There is a similar pattern of distributions to those of the reported frequency datasets (Figure 6). The model of Kadib (1965) predicts reduced levels of transport compared to other models and Lettau and Lettau (1977) produces widely a distributed pattern for the wind tunnel datasets. The Bagnold (1936) model shows consistency for both wind tunnel and reported frequency datasets.

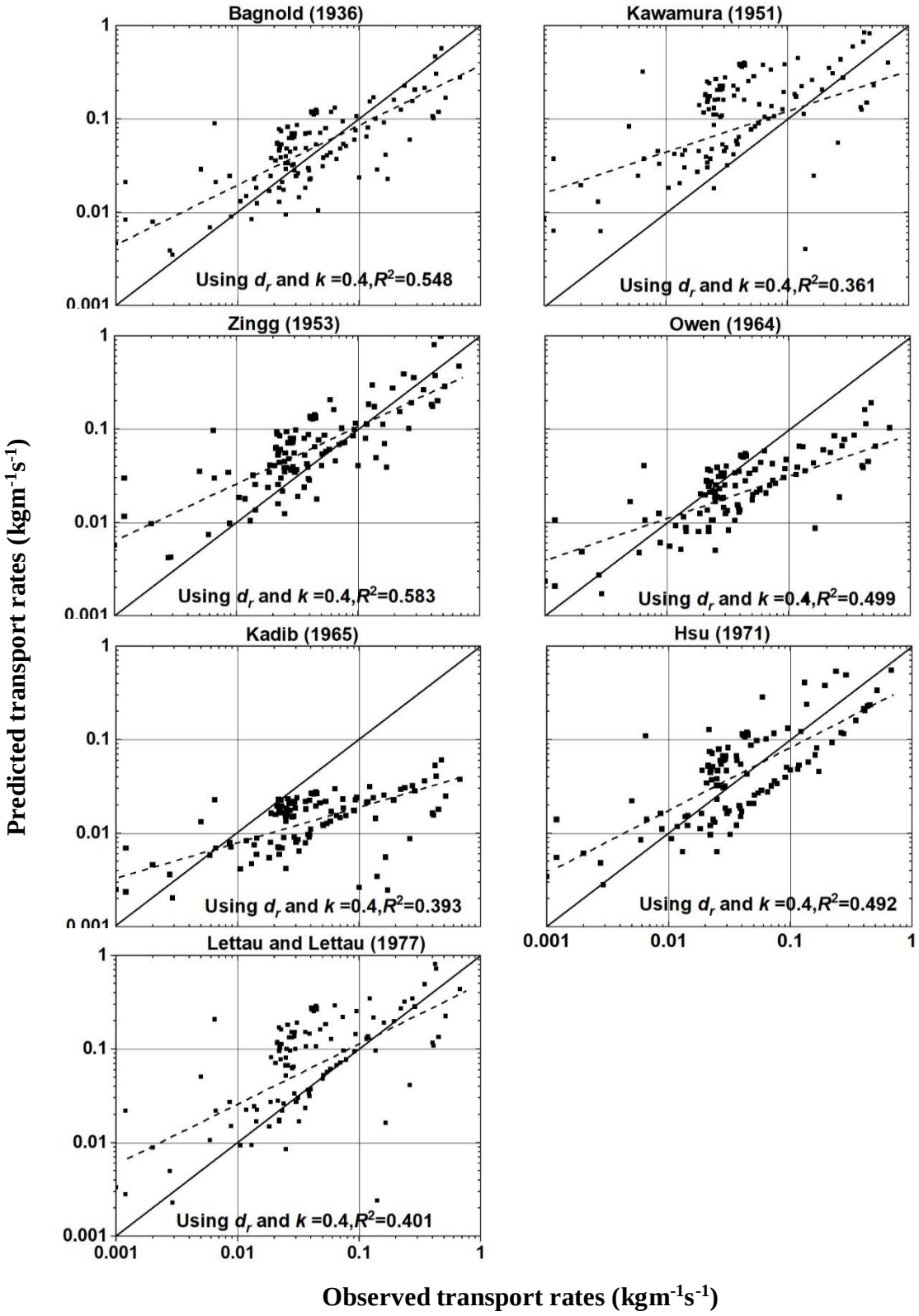

Figure 7: Comparison of observed and predicted rates with d_r, wind tunnel datasets.

The data of Kubota et al. (1982), Berg (1983), Butterfield (1991), Sherman et al. (1998) were collected in the field. These experiments contain a total of 123 observed aeolian transport rates ranging between 0.00001 to 0.08 $kgm^{-1}s^{-1}$. The results of the transformation of mean grain diameter are given in Table 10. The scatter distributions of the observed and predicted rates of field datasets are plotted in Figure 8.

Table 10: Results of regression analysis of field data with original (d_{50}) and converted mean diameter (d_r) and k=0.4.

Results from d_{50} and k =0.4 (Field Studies)								
Models	Bagnold	Kawamura	Zingg	Owen	Lettau	Hsu	Kadib	Average
R^2	0.625	0.607	0.556	0.709	0.661	0.511	0.639	0.615
RMSE	0.010	0.020	0.005	0.005	0.017	0.015	0.003	0.011
A	0.011	0.017	0.005	0.005	0.01	0.015	0.006	0.01
B	1.131	2.104	0.521	0.624	1.956	0.643	0.379	1.051
Results from d_r and k=0.4 (Field Studies)								
Models	Bagnold	Kawamura	Zingg	Owen	Lettau	Hsu	Kadib	Average
R^2	0.631	0.603	0.571	0.683	0.659	0.551	0.631	0.615
RMSE	0.011	0.0315	0.015	0.005	0.022	0.017	0.004	0.015
A	0.012	0.026	0.015	0.006	0.012	0.015	0.006	0.013
B	1.164	3.430	1.432	0.645	2.487	0.622	0.388	1.453
Change in R^2	-0.004	-0.004	0.015	-0.026	-0.002	0.04	-0.008	0.003
Change in RMSE	0.006	0.0115	0.01	0.00	0.005	0.002	0.001	0.004
P value	0.000	0.000	0.075	0.114	0.071	0.147	0.000	

Statistically significant improvements are observed in Zingg (1953) and Hsu (1965) models. P values greater than 0.05 in Owen (1964) and Lettau and Lettau (1977) show significant difference between the results of d_{50} and d_r but indicate a decrease in R^2 value. The predictive capability of all aeolian transport models are very close to each other. The lowest and highest R^2 values are observed in the models of Hsu (1971) and Owen (1964) (0.551 and 0.683 respectively), and the values are close to the average value of 0.61. Also, the lowest and highest RMSE values are close to the average value of 0.015.

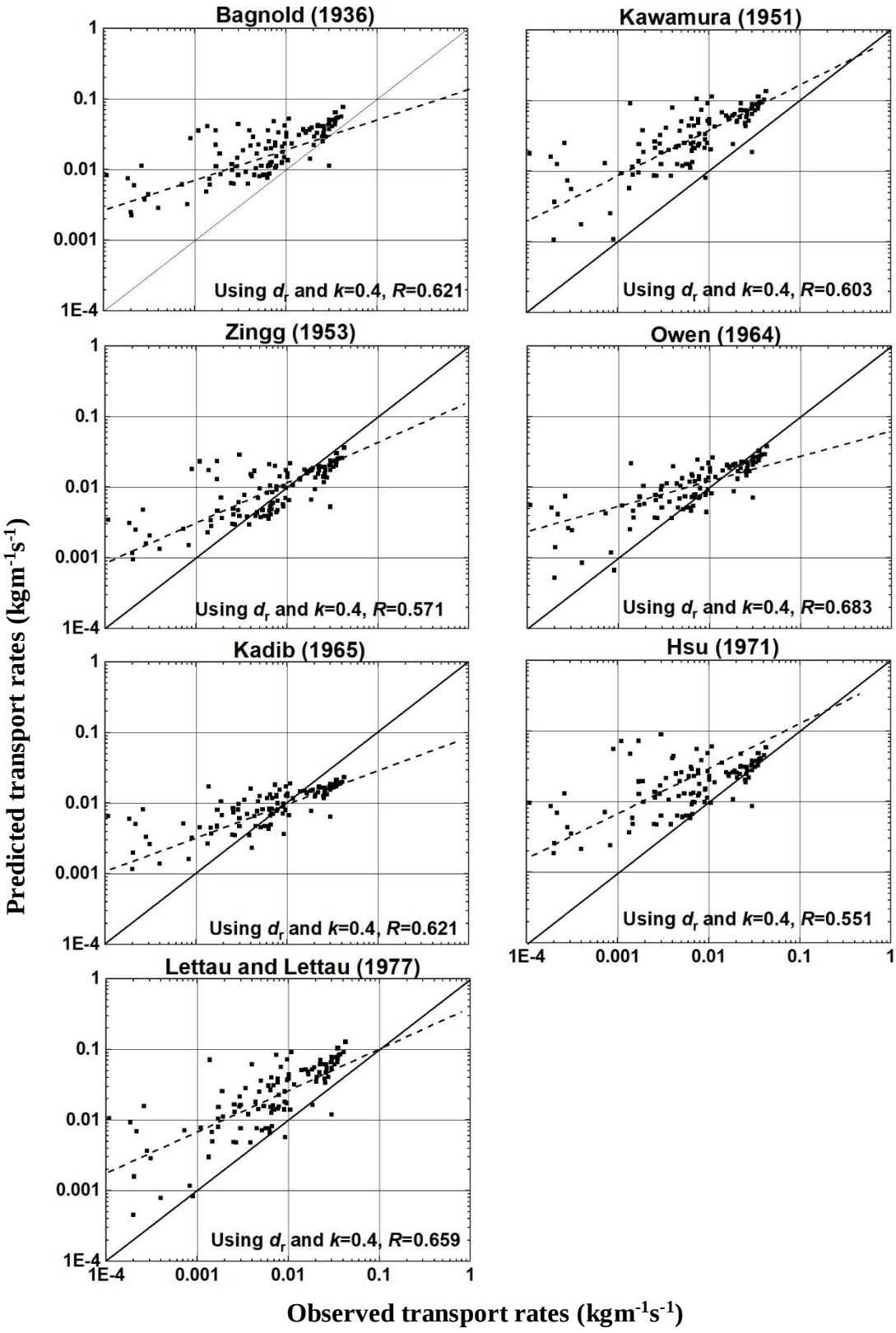

Figure 8: Comparison of observed and predicted rates with d_r, field experimental datasets.

The field datasets produce better results (higher R^2 value and lower RMSE) in terms of the model predictive capabilities. All field-observed transport rates are less than 0.1 $kgm^{-1}s^{-1}$, and it has previously been shown that the models generally performed better at these lower transport rates. Modification of the mean diameter to the mean of mass-weighted distribution brings statistically significant improvement in the predictive capability of Hsu (1971) and Zingg (1953) models for both the wind tunnel and field datasets. Therefore, impact of this modification is consistent both for the wind tunnel and field datasets. Notably, the model of Owen exhibits a significant decrease in predictive capability with the inclusion of d_r.

4.2 Comparative Results of d_{50} and d_r with Apparent von Kármán Parameter (k_a)

To avoid unrealistic values of the apparent von Kármán parameter (k_a), observed transport rates greater than 0.0315 $kgm^{-1}s^{-1}$ were not included in this analysis. This filtering process restricts the value of the apparent von Kármán parameter (k_a) to a range of 0.30-0.40. Statistical results using the apparent von Kármán parameter are summarized in Table 11, and scatter plots of observed and predicted transport rates are shown in Figure 9.

Table 11: Results of regression analysis of the models with apparent von Kármán parameter.

Results from d_{50} and k =0.4								
Model	Bagnold	Kawamura	Zingg	Owen	Lettau	Hsu	Kadib	Average
R^2	0.476	0.543	0.417	0.544	0.513	0.477	0.574	0.506
RMSE	0.007	0.010	0.004	0.004	0.009	0.005	0.002	0.006
A	0.005	0.005	0.002	0.002	0.002	0.004	0.003	0.003
B	1.385	2.394	0.670	0.809	1.957	1.006	0.567	1.255
Results from d_{50} and k_a								
R^2	0.482	0.549	0.415	0.543	0.510	0.483	0.596	0.511
RMSE	0.005	0.009	0.003	0.003	0.007	0.004	0.002	0.005
A	0.005	0.006	0.003	0.003	0.003	0.004	0.003	0.004
B	0.885	1.493	0.430	0.531	1.147	0.637	0.389	0.787
Change in R^2	0.006	0.006	0.002	0.001	-0.003	0.006	0.022	0.005
RMSE change	-0.002	-0.001	0.001	0.001	-0.002	0.001	0.000	-0.001
P (d_{50}/k_a)	0.000	0.000	0.000	0.000	0.000	0.085	0.114	

(Table 11 continued)

	Results from d_r and k_a							
	Bagnold	Kawamura	Zingg	Owen	Lettau	Hsu	Kadib	Average
R^2	0.491	0.545	0.429	0.545	0.513	0.491	0.601	0.516
RMSE	0.006	0.009	0.003	0.003	0.007	0.004	0.002	0.005
A	0.006	0.005	0.003	0.002	0.003	0.004	0.003	0.004
B	0.913	1.507	0.450	0.556	1.164	0.634	0.391	0.802
Change in R^2	0.015	0.002	0.012	0.001	0.000	0.014	0.027	0.01
RMSE change	-0.001	-0.001	0.001	0.001	-0.002	0.001	0.000	-0.001
P (d_{50}/k_a-d_r)	0.171	0.001	0.074	0.000	0.000	0.134	0.214	

Use of apparent von Kármán parameter (k_a) brings statistically significant improvement in the models of Kadib (1965) and Hsu (1971). The largest improvement in R^2 value occurs in Kadib (1965) model. R^2 value increases from 0.574 to 0.596 and RMSE value remains unchanged. Combined use of mass-weighted mean (d_r) and apparent von Kármán parameter (k_a) brings statistically significant improvement in the models of Bagnold (1936), Zingg (1953), Hsu (1971), and Kadib (1965). The largest improvement is observed in Kadib (1965) where R^2 value changes from 0.574 to 0.592 and RMSE value remains unchanged.

Lower transport rates are predicted by most of the models after incorporation of the use of mass-weighted mean (d_r) and apparent von Kármán parameter (k_a) (Figure 9), although Figure 8 does indicate significant overprediction in the models of Kawamura (1951) and Bagnold (1936). Comparison of Figure 9 with the others (Figure 6 and 7) demonstrates the effectiveness of the modified approaches in reducing the difference between observed and predicted rates. However, it should be noted that use of the apparent von Kármán constant requires elimination of the highest observed transport rates, which most of the models underpredicted.

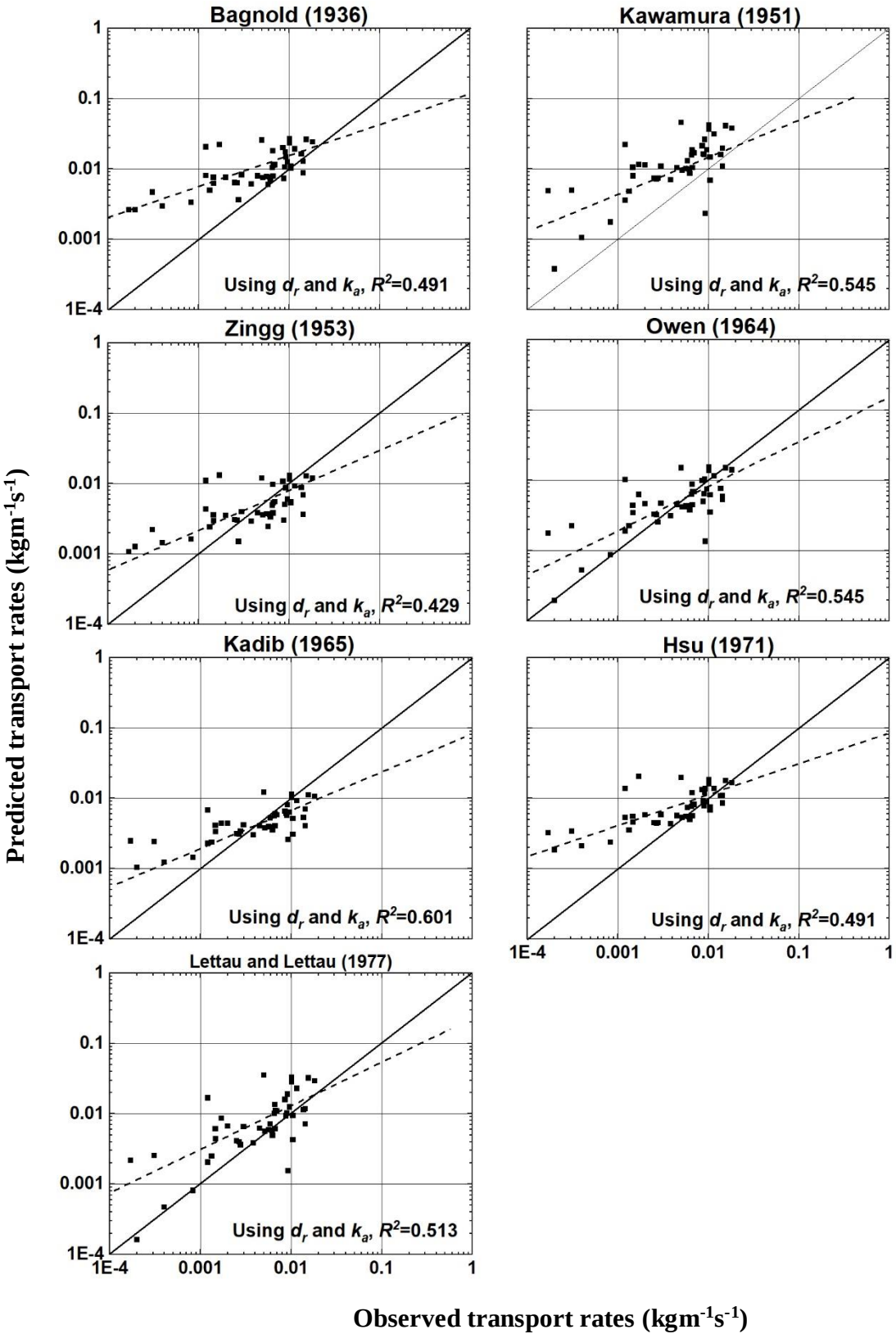

Figure 9: Comparison of observed and predicted rates with d_r and k_a.

4.3 Comparative Results of d_{50} and d_r with Recalibrated Empirical Coefficients

The recalibrated empirical coefficients determined from best-fits for both reported frequency (C_R) and estimated frequency (C_E) datasets are summarized in Table 12, along with the original coefficients (C_o). Regression analyses were conducted separately for both reported frequency and estimated frequency datasets using recalibrated coefficients (Table 13). Note that the R^2 values are identical for both the original and recalibrated coefficients in all the models, but RMSE values are reduced or remain same. This is because R^2 is computed as a ratio of the regression sum of squares and the total sum of squares. In comparison, RMSE is determined from the differences between that values predicted by a model and the observed values. Therefore, RMSE value would be different for each coefficient.

Table 12: Summary of empirical coefficients for the transport rates.

Constant	**Bagnold**	**Kawamura**	**Zingg**	**Lettau and Lettau**
C_o	1.8	2.78	0.83	4.2
C_R	2.99	2.84	0.84	4.39
C_E	2.70	2.41	2.66	4.39

Table 13: Results of regression analysis of the models with recalibrated empirical coefficients and converted mean grain diameter.

Results from d_r and original coefficients (Reported frequency datasets)					
Models	Bagnold	Kawamura	Zingg	Lettau and Lettau	Average
R^2	0.525	0.226	0.595	0.368	0.429
RMSE	0.045	0.067	0.027	0.080	0.055
A	0.028	0.059	0.012	0.045	0.036
B	0.482	0.370	0.333	0.615	0.450
Results from d_r and calibrated coefficients (Reported frequency datasets)					
R^2	0.525	0.226	0.595	0.368	0.429
RMSE	0.036	0.067	0.025	0.077	0.051
A	0.046	0.058	0.011	0.044	0.040
B	0.803	0.369	0.332	0.615	0.530
Change in R^2	0.000	0.000	0.000	0.000	0.000
Change in RMSE	-0.009	0.000	-0.002	-0.003	-0.004

(Table 13 continued)

Results from d_r and original coefficients (Estimated frequency datasets)					
Models	Bagnold	Kawamura	Zingg	Lettau	Average
R^2	0.908	0.918	0.892	0.905	0.906
RMSE	0.015	0.007	0.007	0.029	0.015
A	0.014	0.006	0.005	0.017	0.011
B	0.607	0.287	0.239	1.139	0.568
Results from d_r and calibrated coefficients (Estimated frequency datasets)					
R^2	0.908	0.918	0.892	0.905	0.906
RMSE	0.012	0.007	0.0066	0.0286	0.014
A	0.020	0.014	0.018	0.018	0.018
B	0.91	0.314	0.918	1.190	0.833
Change in R^2	0.000	0.000	0.000	0.000	0.000
Change in RMSE	-0.003	0.00	-0.0004	-0.0004	-0.001

On average, recalibration of the empirical coefficients reduces the RMSE by about 8% with reported frequency distributions and 7% for those which were estimated. The largest reductions in RMSE by far occur with the Bagnold (1936) model which shows about 20% decrease in RMSE in both cases. This underscores the complication of using a fixed empirical coefficient for a range of environmental conditions. The empirical coefficient changes only a small amount for the Kawamura (1951) and Lettau and Lettau (1977) model. Therefore, the original empirical coefficient of Kawamura (1951) and Lettau and Lettau (1977) model fit the datasets used in this study reasonably well. The recalibrated coefficients for Bagnold (1936) were more than 50% larger than the original.

4.4 Discussion of the Results

Use of the mass-weighted mean grain size produces improvement in goodness of fit in a majority. The R^2 value for reported frequency datasets increases 16.5% for the Hsu (1971) model. Substantial improvements are also noted with Kadib (1965) (about 9.1%) and Zingg (1953) (about 4.2%). All these improvements are statistically significant with 5% level of significance. Both the

Hsu (1971) and Kadib (1965) models use a secondary equation to define their coefficients (Equation 11 and 8) rather than employing a constant. Therefore, the empirical coefficients of the above two models depend directly on the grain size and shear velocity for each run. This dependency could be the reason that Hsu (1971) and Kadib (1965) model are more sensitive to grain size and provide better results for the larger datasets employed here. The model of Kadib (1965) shows improvement both for the reported and estimated frequency datasets and demonstrates its sensitivity to the small change of grain diameter for all types of data. Improvement also occurs in the model of Zingg (1953).

The predictive capability of all aeolian transport models is very close to each other for the field datasets (Figure 8). In this case, all of the field-measured transport rates are less than 0.1 $kgm^{-1}s^{-1}$ and the transport models appear to better address lower transport rates. Use of the mass-weighted mean grain size brings improvement in predictive capability of Hsu (1971) and Zingg (1953) for both the wind tunnel and field datasets. Therefore, the impact of the modification approach is consistent for both the wind tunnel and field datasets. The Hsu (1971) model consistently shows improvement with the mass-weighted mean even for the larger grain sizes.

Lower transport rates are predicted by most of the models after incorporation of the use of mass-weighted mean (d_r) and apparent von Kármán parameter (k_a). Figure 10 depicts the relationship of observed and predicted transport rates for the Bagnold (1936) model applying both modification. Consequently, the gap between observed and predicted rates can be reduced from about an order of magnitude to about a quarter of an order of magnitude by the combined use of the above two modified approaches. There is an overall reduction in predicted transport after the modifications. This reduction increases exponentially for the higher transport rates, correction alone would make the predictions much closer to observations. However, it should be noted that

use of the apparent von Kármán constant requires elimination of the highest observed transport rates, which most of the models underpredicted.

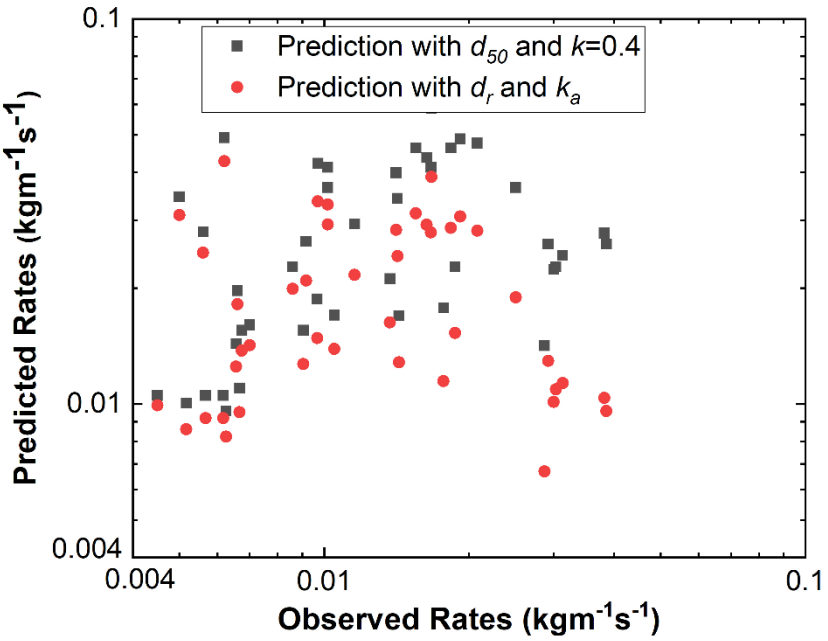

Figure 10: Comparison of the performance of the Bagnold (1936) model using its original configuration with the von Kármán constant, and after change with the apparent von Kármán parameter and mean of the mass weighted distribution.

Use of mass-weighted mean and the apparent von Kármán parameter produces the strongest improvements in the model of Hsu (1971), Kadib (1965) and Bagnold (1936) as these models are sensitive to the change in mean diameter. As the apparent von Kármán parameter produces reduced level of shear velocity, all the models predict lower transport rates, producing better agreement with observed transport.

CHAPTER 5: SUMMARY AND CONCLUSION

This study incorporated the mean of the mass-weighted frequency distribution along with a transport dependent apparent von Kármán parameter in commonly used models of aeolian transport rates. A large set of previously reported experimental data was assembled to test the utility of the above modifications. From the analysis, the following outcomes were derived.

1. Most of the models show improvement in prediction of transport rates when the mean diameter is transformed to a mass-weighted mean with an average of 4% and a maximum of 16.5%.

2. The study indicates that the Hsu (1971) and Kadib (1965) models are most improved by inclusion of the mass-weighted mean (16.5% and 9.1% respectively). Moreover, the Zingg (1953) model was found to best replicate the observed transport rates, and showed an improvement in R^2 value from 0.57 to 0.59 with inclusion of the mass-weighted mean for reported frequency datasets.

3. Use of apparent von Kármán parameter along with the mean of the mass-weighted distribution slightly reduces the gap between observed and predicted transport rates. With this modification, the Kadib (1965) model showed the best results in replicating observed transport rates However, this approach is not applicable for transport rates greater than 0.0315 $kgm^{-1}s^{-1}$, so it is of limited utility

4. The recalibration process provides further improvement in reducing gap between the observed and predicted rates by providing lower RMSE values.

The results of this study indicate that the overall performance of the aeolian transport models is generally improved with the tested modifications. These results, however, do not demonstrate the uncritical applicability of these models. As discussed, there are many potential site-specific complications that are not addressed in these models. For environments with any of these confounding factors it is to be expected that substantial differences between measured and predicted aeolian transport rates will continue to be the case. However, this study will help to move forward the general applicability of wind blown sediment transport models.

REFERENCES

Anderson, R. S., & Hallet, B. (1986). Sediment transport by wind: toward a general model. *Geological Society of America Bulletin, 97*(5), 523-535.

Armbrust, D., & Retta, A. (2000). Wind and sandblast damage to growing vegetation. *Annals of Arid Zone, 39*(3), 273-284.

Arnold, S. (2002). Development of the saltation system under controlled environmental conditions. *Earth Surface Processes and Landforms, 27*(8), 817-829.

Atherton, R. J., Baird, A. J., & Wiggs, G. F. (2001). Inter-tidal dynamics of surface moisture content on a meso-tidal beach. *Journal of coastal research*, 482-489.

Baas, A. C. (2007). Complex systems in aeolian geomorphology. *Geomorphology, 91*(3), 311-331.

Bagnold, R. (1936). The movement of desert sand. *Proceedings of the Royal Society of London. Series A, Mathematical and Physical Sciences, 157*(892), 594-620.

Bagnold, R. (1937). The transport of sand by wind. *The Geographical Journal, 89*(5), 409-438.

Bagnold, R. (1941). The physics of blown sand and desert dunes: Methuen and Co. Ltd., London, 265 p., 1956, The flow of cohesionless grains in fluids. *Phil. Trans. Roy. Soc. London, Set. A, 249*, 235-297.

Barrere, J., Gipouloux, O., & Whitaker, S. (1992). On the closure problem for Darcy's law. *Transport in Porous Media, 7*(3), 209-222.

Bauer, B. O., Davidson-Arnott, R. G., Nordstrom, K. F., Ollerhead, J., & Jackson, N. L. (1996). Indeterminacy in aeolian sediment transport across beaches. *Journal of Coastal Research*, 641-653.

Bauer, B., Houser, C., & Nickling, W. (2004). Analysis of velocity profile measurements from wind-tunnel experiments with saltation. *Geomorphology, 59*(1), 81-98.

Bauer, B. O. (2009). Contemporary research in aeolian geomorphology. *Geomorphology, 105*(1), 1-5.

Bauer, B., Davidson-Arnott, R., Hesp, P., Namikas, S., Ollerhead, J., & Walker, I. (2009). Aeolian sediment transport on a beach: Surface moisture, wind fetch, and mean transport. *Geomorphology, 105*(1), 106-116.

Belly, Pierre-Yves. Sand movement by wind. No. S-72-I-7. California Univ Berkeley Inst of Engineering Research, 1962.

Belly, P.-Y. (1964). Sand movement by wind: US Army. *Coastal Eng. Research Center, Tech. Memo. I.*

Berg, N. H. (1983). Field evaluation of some sand transport models. *Earth Surface Processes and Landforms, 8*(2), 101-114.

Butterfield, G. (1991). Grain transport rates in steady and unsteady turbulent airflows. In *Aeolian Grain Transport 1* (pp. 97-122): Springer.

Chapman, D. M. (1990). Aeolian sand transport—an optimized model. *Earth Surface Processes and Landforms, 15*(8), 751-760.

Chen, W., & Fryrear, D. W. (2001). Aerodynamic and geometric diameters of airborne particles. *Journal of Sedimentary Research, 71*(3), 365-371.

Cornelis, W. M., Gabriels, D., & Hartmann, R. (2004). A parameterization for the threshold shear velocity to initiate deflation of dry and wet sediment. *Geomorphology, 59*(1-4), 43-51.

Crickmore, M., & Lean, G. (1962). The measurement of sand transport by means of radioactive tracers. *Proc. R. Soc. Lond. A, 266*(1326), 402-421.

Cornelis, W., & Gabriels, D. (2003). The effect of surface moisture on the entrainment of dune sand by wind: an evaluation of selected models. *Sedimentology, 50*(4), 771-790.

Crickmore, M. (1967). Measurement of sand transport in rivers with special reference to tracer methods. *Sedimentology, 8*(3), 175-228.

Davidson-Arnott, R., & Bauer, B. (2009). Aeolian sediment transport on a beach: thresholds, intermittency, and high frequency variability. *Geomorphology, 105*(1), 117-126.

Dong, Z., Liu, X., Wang, H., & Wang, X. (2003). Aeolian sand transport: a wind tunnel model. *Sedimentary Geology, 161*(1-2), 71-83.

Dong, Z., Wang, H., Liu, X., & Wang, X. (2004). A wind tunnel investigation of the influences of fetch length on the flux profile of a sand cloud blowing over a gravel surface. *Earth Surface Processes and Landforms, 29*(13), 1613-1626.

Draga, M. (1983). Eolian activity as a consequence of beach nourishment-observations at Westerland (Sylt), German North Sea coast. *Zeitschrift für Geomorphologie*, 303-319.

Edwards, B. L., & Namikas, S. L. (2015). Characterizing the sediment bed in terms of resistance to motion: Toward an improved model of saltation thresholds for aeolian transport. *Aeolian Research, 19*, 123-128.

Einstein, H. A. (1950). The bed-load function for sediment transportation in open channel flows (Vol. 1026): Citeseer.

Ellis, J. T., Sherman, D. J., Farrell, E. J., & Li, B. (2012). Temporal and spatial variability of aeolian sand transport: Implications for field measurements. *Aeolian Research, 3*(4), 379-387.

Farrell, E., & Sherman, D. (2006). Process-scaling issues for aeolian transport modelling in field and wind tunnel experiments: Roughness length and mass flux distributions. *Journal of coastal research*, 384-389.

Field, J. P., Belnap, J., Breshears, D. D., Neff, J. C., Okin, G. S., Whicker, J. J., . . . Reynolds, R. L. (2010). The ecology of dust. *Frontiers in Ecology and the Environment, 8*(8), 423-430.

Fryrear, D., & Downes, J. (1975). Estimating seedling survival from wind erosion parameters. *Transactions of the ASAE, 18*(5), 888-0891.

Fryrear, D. W. (1981). Long-term effect of erosion and cropping on soil productivity. *Geological Society of America*, 186, 253-259.

Fryrear, D. (1987). Aerosol measurements from 31 dust storms. *Ariman* T, Veziroglu T N. Particulate and Multiphase Flows: Contamination Analysis. and Control. *New York: Hemisphere Publishing Corp*, 407-415.

Gares, P. A., Sherman, D. J., & Nordstrom, K. F. (1994). Geomorphology and natural hazards. In *Geomorphology and natural hazards* (pp. 1-18): Elsevier.

Gerety, K. (1985). Problems with determination of u_* from wind-velocity profiles measured in experiments with saltation. Paper presented at the Proceedings of international workshop on the physics of blown sand.

Granja, H., & de Carvalho, G. S. (1992). Dunes and Holocene deposits of the coastal zone north of Mondego Cape, Portugal.

Haff, P. K., & Presti, D. E. (1995). Barchan dunes of the Salton Sea region, California. In *Desert Aeolian Processes* (pp. 153-177): Springer.

Herrmann, H., & Sauermann, G. (2000). The shape of dunes. *Physica A: Statistical Mechanics and its Applications, 283*(1-2), 24-30.

Hesp, P. (1981). The formation of shadow dunes. *Journal of Sedimentary Research, 51*(1).

Hesp, P. A., Davidson-Arnott, R., Walker, I. J., & Ollerhead, J. (2005). Flow dynamics over a foredune at Prince Edward Island, Canada. *Geomorphology, 65*(1), 71-84.

Horikawa, K., & Shen, H. W. (1960). Sand movement by wind action (on the characteristics of sand traps) (No. TM119). *Coastal Engineering Research Center Vicksburg MS*.

Horikawa, K., Hotta, S., Kubota, S., & Katori, S. (1983). On the sand transport rate by wind on a beach. *Coastal Engineering in Japan, 26*(1), 101-120.

Horikawa, K., Hotta, S., & Kraus, N. C. (1986). Literature review of sand transport by wind on a dry sand surface. *Coastal Engineering, 9*(6), 503-526.

Hsu, S. A. (1971). Wind stress criteria in eolian sand transport. *Journal of Geophysical Research, 76*(36), 8684-8686.

Huang, N., Wang, C., & Pan, X. (2010). Simulation of aeolian sand saltation with rotational motion. *Journal of Geophysical Research: Atmospheres, 115*(D22).

Iversen, J. D., & Rasmussen, K. R. (1999). The effect of wind speed and bed slope on sand transport. *Sedimentology, 46*(4), 723-731.

Jackson, N., & Nordstrom, K. (1997). Field investigation of the effects of surface drying on sediment transport rates across a beach, Wildwood, New Jersey, USA. *Earth Surface Processes and Landforms, 22*, 611-621.

Kadib, A. L. (1963). Beach profile as affected by vertical walls (No. DA-49-055-CE-634). California Univ Berkeley Hydraulic Engineering Lab.

Kadib, A. A. (1965). A function for sand movement by wind (No. HEL-2-12). California Univ Berkeley Hydraulic Engineering Lab.

Kawamura, R. (1951). Study on sand movement by wind(Relationship between sand flow and wind friction, and vertical density distribution of sand). *Tokyo Daigaku Rikogaku Kenkyusho Hokoku,(Tokyo), 5*(3), 95-112.

Kellogg, F. (1915). Sand-dune reclamation on the coast of northern California and southern Oregon. *Soc. Amer. For. Proc, 10*, 41-64.

Kok, J. F., Parteli, E. J., Michaels, T. I., & Karam, D. B. (2012). The physics of wind-blown sand and dust. *Reports on Progress in Physics, 75*(10), 106901

Kok, J., Mahowald, N., Albani, S., Fratini, G., Gillies, J., Ishizuka, M., . . . Park, S.-U. (2014). An improved dust emission model with insights into the global dust cycle's climate sensitivity. *Atmospheric Chemistry & Physics*, *14*(5).

Kubota, S., Horikawa, K., & Hotta, S. (1982). Blown sand on beaches *Coastal Engineering 1982* (pp. 1181-1198).

Kuriyama, Y., Mochizuki, N., & Nakashima, T. (2005). Influence of vegetation on aeolian sand transport rate from a backshore to a foredune at Hasaki, Japan. *Sedimentology, 52*(5), 1123-1132.

Kuriyama, Y., Mochizuki, N., & Nakashima, T. (2005). Influence of vegetation on aeolian sand transport rate from a backshore to a foredune at Hasaki, Japan. *Sedimentology, 52*(5), 1123-1132.

Lal, R. (1988). Soil degradation and the future of agriculture in sub-Saharan Africa. *Journal of Soil and Water Conservation, 43*(6), 444-451.

Lancaster, N., & Baas, A. (1998). Influence of vegetation cover on sand transport by wind: field studies at Owens Lake, California. *Earth Surface Processes and Landforms, 23*(1), 69-82.

Leatherman, S. (1978). A new aeolian sand trap design. *Sedimentology, 25*(2), 303-306.

Leenders, J. K., Sterk, G., & Van Boxel, J. H. (2011). Modelling wind-blown sediment transport around single vegetation elements. *Earth Surface Processes and Landforms, 36*(9), 1218-1229.

Lettau, K., & Lettau, H. (1977). Experimental and micrometeorological field studies of dune migration.

Li, B., Granja, H., Farrell, E. J., Ellis, J. T., & Sherman, D. J. (2009). Aeolian saltation at Esposende Beach, Portugal. *Journal of coastal research*, 327-331.

Li, B., Sherman, D. J., Farrell, E. J., & Ellis, J. T. (2010). Variability of the apparent von Kármán parameter during aeolian saltation. *Geophysical Research Letters, 37*(15).

Liu, X., Dong, Z., & Wang, X. (2006). Wind tunnel modeling and measurements of the flux of wind-blown sand. *Journal of arid environments, 66*(4), 657-672.

Logie, M. (1981). Wind tunnel experiments on dune sands. *Earth Surface Processes and Landforms, 6*(3-4), 365-374.

Madore, C., & Leatherman, S. (1981). Dune stabilization of the Provincelands, Cape Cod National Seashore. *Report for the Environmental Institute at the University of Massachusetts, Amherst, MA*.

McEwan, I., & Willetts, B. (1994). On the prediction of bed-load sand transport rate in air. *Sedimentology, 41*(6), 1241-1251.

McKee, E. D. (1966). Structures of dunes at White Sands National Monument, New Mexico (and a comparison with structures of dunes from other selected areas). *Sedimentology, 7*(1), 3-69.

McKenna Neuman, C., & Langston, G. (2006). Measurement of water content as a control of particle entrainment by wind. *Earth Surface Processes and Landforms, 31*(3), 303-317.

Michels, K., Sivakumar, M., & Allison, B. (1995). Wind erosion control using crop residue I. Effects on soil flux and soil properties. *Field Crops Research, 40*(2), 101-110.

Middleton, N. J., & Thomas, D. S. (1992). World atlas of desertification.

Mulligan, K. R. (1988). Velocity profiles measured on the windward slope of a transverse dune. *Earth Surface Processes and Landforms, 13*(7), 573-582.

Namikas, S. L., & Sherman, D. J. (1995). A review of the effects of surface moisture content on aeolian sand transport *Desert aeolian processes* (pp. 269-293): Springer.

Namikas, S. L. (2003). Field measurement and numerical modeling of aeolian mass flux distributions on a sandy beach. *Sedimentology, 50*(2), 303-326.

Neuman, C. M. (2003). Effects of temperature and humidity upon the entrainment of sedimentary particles by wind. *Boundary-Layer Meteorology, 108*(1), 61-89.

Nickling, W. (1988). The initiation of particle movement by wind. *Sedimentology, 35*(3), 499-511.

Nickling, W. G., & Davidson-Arnott, R. G. (1990). BEACHES AND COASTAL SAND DUNES. Paper presented at the Proceedings Canadian Symposium on Coastal Sand Dunes.

Niedoroda, A. W., Sheppard, D. M., & Devereaux, A. B. (1991). The effect of beach vegetation on aeolian sand transport. Paper presented at the Coastal Sediments.

O'brien, M., & Rindlaub, B. (1936). The transportation of sand by wind. *Civil Engineering, 6*(5), 325-327.

Owen, P. R. (1964). Saltation of uniform grains in air. *Journal of Fluid Mechanics, 20*(2), 225-242.

Ravi, S., Zobeck, T. M., Over, T. M., Okin, G. S., & D'ODORICO, P. (2006). On the effect of moisture bonding forces in air-dry soils on threshold friction velocity of wind erosion. *Sedimentology, 53*(3), 597-609.

Rinaudo, T. (1996). Tailoring wind erosion control methods to farmers' specific needs. *Wind Erosion in West Africa: The Problem and its Control*, 161-171.

Rosen, P. (1978). An efficient, low cost, aeolian sampling system. *Geological Survey of Canada, Current Research, Part A, 781*, 531-532.

Sarre, R. (1988). Evaluation of aeolian sand transport equations using intertidal zone measurements, Saunton Sands, England. *Sedimentology, 35*(4), 671-679.

Schönfeldt, H. J. (2004). Establishing the threshold for intermittent aeolian sediment transport. *Meteorologische Zeitschrift, 13*(5), 437-444.

Sherman, D. J., & Nordstrom, K. F. (1994). Hazards of wind-blown sand and coastal sand drifts: a review. *Journal of coastal research*, 263-275.

Sherman, D. J., Jackson, D. W., Namikas, S. L., & Wang, J. (1998). Wind-blown sand on beaches: an evaluation of models. *Geomorphology, 22*(2), 113-133.

Sherman, D. J., & Farrell, E. J. (2008). Aerodynamic roughness lengths over movable beds: Comparison of wind tunnel and field data. *Journal of Geophysical Research: Earth Surface, 113*(F2).

Sherman, D. J., & Li, B. (2012). Predicting aeolian sand transport rates: A reevaluation of models. *Aeolian Research, 3*(4), 371-378.

Sherman, D. J., Li, B., Ellis, J. T., Farrell, E. J., Maia, L. P., & Granja, H. (2013). Recalibrating aeolian sand transport models. *Earth Surface Processes and Landforms, 38*(2), 169-178.

Stout, J., & Zobeck, T. (1997). Intermittent saltation. *Sedimentology, 44*(5), 959-970.

Skidmore, E. (1966). Wind and Sandblast Injury to Seedling Green Beans1. *Agronomy Journal, 58*(3), 311-315.

Sterk, G. (2000). Flattened residue effects on wind speed and sediment transport. *Soil Science Society of America Journal, 64*(3), 852-858.

Sterk, G. (2003). Causes, consequences and control of wind erosion in Sahelian Africa: a review. Land Degradation & Development, 14(1), 95-108.

Svasek, J., & Terwindt, J. (1974). Measurements of sand transport by wind on a natural beach. *Sedimentology, 21*(2), 311-322.

Tsoar, H. (1983). Wind tunnel modeling of echo and climbing dunes. In *Developments in Sedimentology* (Vol. 38, pp. 247-259): Elsevier.

UNEP, 1999 UNEP, 1999. Dioxin and furan inventories – national and regional emissions of PCDD/PCDF. In: Fiedler, H., *Report by UNEP Chemicals*, Geneva, Switzerland. May 1999.

White, B. R., & Tsoar, H. (1998). Slope effect on saltation over a climbing sand dune. *Geomorphology, 22*(2), 159-180.

Wiggs, G., Atherton, R., & Baird, A. (2004). Thresholds of aeolian sand transport: establishing suitable values. *Sedimentology, 51*(1), 95-108.

Wippermann, F., & Gross, G. (1986). The wind-induced shaping and migration of an isolated dune: a numerical experiment. *Boundary-Layer Meteorology, 36*(4), 319-334.

Wolfe, S. A., & Nickling, W. G. (1993). The protective role of sparse vegetation in wind erosion. *Progress in physical geography, 17*(1), 50-68.

Woodhouse, W. W. (1978). Dune building and stabilization with vegetation: The Center.

Yang, Y., & Davidson-Arnott, R. G. (2005). Rapid measurement of surface moisture content on a beach. *Journal of coastal research*, 447-452.

Zingg, A. (1953). Wind tunnel studies of the movement of sedimentary material. Paper presented at the Proceedings of the 5th Hydraulic Conference Bulletin.

APPENDIX A: DATA COLLECTED FROM THE LITERATURE (REPORTED FREQUENCY DATASETS)

Sl. No.	Study	d_{50} (mm)	d_r (mm)	u_* (ms^{-1})	Q ($kgm^{-1}s^{-1}$)
1	Belly (1962)	0.44	0.46	0.39	0.0143
2				0.41	0.0012
3				0.41	0.0066
4				0.42	0.0137
5				0.43	0.0086
6				0.43	0.0303
7				0.43	0.0187
8				0.44	0.0313
9				0.45	0.0292
10				0.45	0.0386
11				0.46	0.0382
12				0.5	0.0505
13				0.51	0.0545
14				0.52	0.0580
15				0.54	0.0700
16				0.55	0.0780
17				0.58	0.0910
18				0.64	0.1180
19				0.3	0.0012
20				0.35	0.0105
21				0.38	0.0182
22				0.39	0.0220
23				0.41	0.0232
24				0.46	0.0380
25				0.5	0.0506
26	Belly (1962)	0.3	0.32	0.16	0.0000
27				0.33	0.0250
28				0.38	0.0320
29				0.41	0.0360
30				0.44	0.0390
31				0.49	0.0500
32				0.59	0.0740
33				0.66	0.0930

(Appendix A Continued)

Sl. No.	Study	d_{50} (mm)	d_r (mm)	u_* (ms^{-1})	Q ($kgm^{-1}s^{-1}$)
34	Kadib Sand C (1963)	0.14	0.16	0.22	0
35				0.244	0.00017
36				0.278	0.00277
37				0.336	0.0059
38				0.368	0.0088
39				0.41	0.0144
40				0.595	0.0189
41				0.626	0.027
42				0.645	0.0365
43				0.73	0.0475
44				0.76	0.053
45				0.79	0.00649
46				0.805	0.0736
47				0.84	0.095
48	Kadib Sand D (1965)	1	1.12	0.391	0.01
49				0.49	0.023
50				0.62	0.052
51				0.6	0.14
52				0.71	0.13
53				0.79	0.149
54				0.7	0.18
55				0.77	0.28
56				1	0.422
57				1.08	0.475
58	Kadib Sand E (1965)	0.88	1	0.19	0.0005
59				0.29	0.049
60				0.38	0.1
61				0.37	0.165
62				0.4	0.48
63				0.45	0.16
64				0.51	0.2523
65				0.61	0.403
66				0.62	0.4
67				0.64	0.45
68				0.73	0.508
69				0.85	0.675

(Appendix A Continued)

Sl. No.	Study	d_{50} (mm)	d_r (mm)	u_* (ms^{-k1})	Q ($kgm^{-1}s^{-1}$)
70	Kubota et al. (1982)	0.14	0.16	0.22	0.00
71		0.27	0.3	0.23	0.0004
72				0.22	0.0002
73				0.24	0.000833
74				0.275	0.001333
75				0.301	0.0025
76				0.3	0.002667
77		0.267	0.296	0.3	0.003833
78				0.33	0.003
79				0.33	0.0045
80				0.325	0.005167
81				0.33	0.005667
82				0.33	0.006167
83				0.32	0.00625
84				0.335	0.006667
85				0.38	0.007
86				0.4	0.009667
87		0.3	0.32	0.38	0.0105
88				0.44	0.009167
89				0.49	0.010167
90				0.49	0.025
91				0.51	0.010167
92				0.51	0.016667
93				0.52	0.016333
94				0.53	0.0155
95				0.53	0.018333
96				0.54	0.019167
97	Namikas (2003)	0.25	0.28	0.27	0.00031
98				0.32	0.00146
99				0.32	0.00006
100				0.37	0.00656
101				0.3	0.00147
102				0.38	0.00905
103				0.38	0.00674
104				0.47	0.01157
105				0.63	0.04054
106	Huang et al. (2006)	0.228	0.26	0.325	0.002
107				0.5	0.005
108				0.675	0.039
109				0.83	0.063

(Appendix A continued)

Sl. No.	Study	d_{50} (mm)	d_r (mm)	u_* (ms^{-1})	Q ($kgm^{-1}s^{-1}$)
110	Butterfield (1991), Wind Tunnel	0.177	0.2	0.56	0.0205
111				0.61	0.022
112				0.625	0.0222
113				0.58	0.025
114				0.675	0.028
115				0.75	0.0307
116				0.64	0.0223
117				0.64	0.023
118				0.675	0.0282
119				0.715	0.0228
120				0.55	0.026
121				0.7	0.0296
122				0.85	0.044
123				0.84	0.0402
124				0.84	0.0427
125				0.83	0.0408
126				0.82	0.0424
127				0.83	0.045
128				0.84	0.0448
129				0.84	0.045
130				0.7	0.036
131				0.725	0.0218
132				0.62	0.0255
133				0.55	0.0248
134				0.675	0.0265
135				0.62	0.0253
136				0.55	0.0249
137				0.645	0.021
138				0.65	0.0212
139				0.64	0.023
140				0.54	0.028
141				0.545	0.029
142				0.83	0.0435
143				0.74	0.0258
144				0.7	0.0278
145				0.68	0.0291
146				0.62	0.0298
147				0.575	0.0225
148				0.675	0.039
149				0.83	0.063

(Appendix A Continued)

Sl. No.	Study	d_{50} (mm)	d_r (mm)	u_* (ms^{-k1})	Q ($kgm^{-1}s^{-1}$)
134	Butterfield (1991), Field Study	0.27	0.29	0.500	0.0205
135				0.560	0.0224
136				0.540	0.03
137				0.570	0.0297
138				0.475	0.0255
139				0.540	0.0265
140				0.600	0.03
141				0.590	0.035
142				0.600	0.0338
143				0.520	0.026
144				0.570	0.0348
145				0.610	0.0362
146				0.560	0.0325
147				0.580	0.0348
148				0.690	0.0425
149				0.590	0.0302
150				0.615	0.0375
151				0.56	0.026
152				0.500	0.0275
153				0.590	0.0302
154				0.565	0.0225
155				0.520	0.022
156				0.560	0.0253
157				0.65	0.0355
158				0.650	0.0348

APPENDIX B: DATA COLLECTED FROM THE LITERATURE (ESTIMATED FREQUENCY DATASETS)

Sl. No.	Study	d_{50} (mm)	d_r (mm)	u_* (ms^{-k1})	Q ($kgm^{-1}s^{-1}$)
1	Bagnold (1936)	0.24	0.247	0.25	0.0029
2				0.404	0.0118
3				0.505	0.0250
4				0.62	0.0440
5				0.88	0.1220
6	Kawamura	0.21	0.27	0.27	0.001
7				0.33	0.013
8				0.36	0.00
9				0.38	0.022
10				0.42	0.024
11				0.46	0.04
12				0.54	0.065
13				0.65	0.115
14				0.73	0.16
15				0.81	0.22
16				0.87	0.275
17				0.97	0.345
18				1.09	0.43
19	Sherman et al. (1998)	0.17	0.204	0.4897	0.00771111
20				0.5068	0.00768889
21				0.3934	0.00540000
22				0.4177	0.00005556
23				0.3425	0.00000556
24				0.4757	0.00689167
25				0.5125	0.00650278
26				0.4097	0.00910278
27				0.3939	0.00026111
28				0.3171	0.00002222
29				0.3908	0.00636111
30				0.4352	0.00784444
31				0.3963	0.00682500
32				0.3423	0.00018333
33				0.2915	0.00001944
34				0.54767	0.01404167
35				0.654	0.01086667
36				0.6054	0.02253056
37				0.4927	0.02020833
38				0.3924	0.00784722

(Appendix B continued)

Sl. No.	Study	d_{50} (mm)	d_r (mm)	u_* (ms^{-k1})	Q ($kgm^{-1}s^{-1}$)
39				0.6069	0.00973333
40				0.5001	0.0097
41				0.3921	0.0029
42				0.2815	0.0000
43				0.5003	0.0000
44				0.6361	0.0073
45				0.5652	0.00831389
46				0.3998	0.00255833
47				0.2876	1.1111E-05
48				0.5788	0.00401667
49				0.4958	0.00502222
50				0.3905	0.00171389
51				0.2518	5.8333E-05
52				0.4497	0.00188333
53				0.3596	0.001925
54				0.6057	0.00136944
55				0.2566	3.0556E-05
56				0.4635	0.00338611
57				0.367	0.00363056
58				0.4282	0.00292778
59				0.3753	0.00256944
60				0.3209	0.00072778
61				0.3541	0.00010833
62				0.4738	0.00601944
63				0.3844	0.00764444
64				0.4481	0.00483333
65				0.3824	0.00469444
66				0.3178	0.00021667
67				0.273	0.00028333
68				0.2785	0.00009444
69				0.2299	0.00020278

VITA

Raihan Jamil received his Bachelor degree in Urban and Regional Planning from Khulna University of Engineering and Technology, Bangladesh in June 2015. Thereafter, he worked as a Research Assistant for six months in a project funded by University Grant Commission (UGC), Bangladesh. Then he worked on another research project funded by South Asian Network for Development and Economics (SANDEE) from December 2015 to July 2016. Currently, he is a graduate student at Louisiana State University, Baton Rouge, USA.